

# LETTER

doi:10.1038/nature13394

---

## Genome sequencing identifies major causes of severe intellectual disability

Christian Gilissen<sup>1\*</sup>, Jayne Y. Hehir-Kwa<sup>1\*</sup>, Djie Tjwan Thung<sup>1</sup>, Maartje van de Vorst<sup>1</sup>, Bregje W. M. van Bon<sup>1</sup>, Marjolein H. Willemsen<sup>1</sup>, Michael Kwint<sup>1</sup>, Irene M. Janssen<sup>1</sup>, Alexander Hoischen<sup>1</sup>, Annette Schenck<sup>1</sup>, Richard Leach<sup>2</sup>, Robert Klein<sup>2</sup>, Rick Tearle<sup>2</sup>, Tan Bo<sup>1,3</sup>, Rolph Pfundt<sup>1</sup>, Helger G. Yntema<sup>1</sup>, Bert B. A. de Vries<sup>1</sup>, Tjitske Kleefstra<sup>1</sup>, Han G. Brunner<sup>1,4\*</sup>, Lisenka E. L. M. Vissers<sup>1\*</sup> & Joris A. Veltman<sup>1,4\*</sup>

**Supplementary Table 1: Detailed cohort description of 50 trios studied by WGS**

Level of ID	Number of patients
IQ <30	31
IQ 30-50	19
IQ 50-70	0

Gender	
Male	26
Female	24

Age Groups	
<10 yrs	26
10-20 yrs	8
>20 yrs	16

Sibship size	
1	4
2	27
3	17
≥4	2

Multiple Congenital Anomalies	
0	27
1	17
2	6

Short Stature	
Yes	15
No	35

Microcephaly	
Yes	18
No	32

Macrocephaly	
Yes	3
No	47

Epilepsy	
Yes	23
No	27

Abnormalities on brain imaging	
Yes	17
No	19
Not assessed	14

Cardiac malformations	
Yes	1
No	49

Abnormalities of the urogenital system	
Yes	11
No	39

**Extended Data Table 2 | *De novo* SNVs of potential clinical relevance identified using WGS**

Trio	Gene	Protein effect	Mutation type	PhyloP <sup>‡</sup>	Gene Classification <sup>§</sup>
1	<i>NGFR</i>	p.(Cys122Arg)	Missense	4.97	-
2	<i>GFPT2</i>	p.(Thr680Ser)	Missense	6.02	-
6	<i>WWP2</i>	p.(Gly10Gly) <sup>†</sup>	Synonymous	-0.12	-
7	<i>TBR1</i>	p.(Gln373Arg)	Missense	3.51	Known
9	<i>WDR45</i>	p.(Cys344Alafs*67)	Frameshift		Known
13	<i>SMC1A</i>	p.(Asn788Lysfs*10)	Frameshift		Known
15	<i>SPTAN1</i>	p.(Glu91Lys)	Missense	5.69	Known
17	<i>ASUN</i>	p.(Gln99*)	Nonsense		-
21	<i>ALG13</i>	p.(Asn107Ser)	Missense	1.34	Known <sup>  </sup>
21	<i>RAI1</i>	p.(Gln88*)	Nonsense		Known
22	<i>MED13L</i>	p.(Asp860Gly)	Missense	4.75	Candidate
24	<i>BRD3</i>	p.(Phe334Ser)	Missense	4.48	-
25	<i>SATB2</i>	p.(Gln310delinsHisCysLysAlaThr)	Insertion		Known
26	<i>PPP2R5D</i>	p.(Trp207Arg)	Missense	5.13	Candidate
27	<i>KCNA1</i>	p.(Thr371Ile)	Missense	5.69	Known
28	<i>SCN2A</i>	p.(Gln1521*)	Nonsense		Known
30	<i>MAST1</i>	p.(Pro1177Arg)	Missense	5.28	-
34	<i>APPL2</i>	p.(Ser329*)	Nonsense		-
41	<i>NACC1</i>	p.(Arg468Cys)	Missense	3.51	-
43	<i>POGZ</i>	p.(Arg1001*)	Nonsense		Candidate
46	<i>TBR1</i>	p.Thr532Argfs*144	Frameshift		Known
49	<i>KANSL2</i>	p.(Gly151Gly) <sup>†</sup>	Synonymous	1.58	Candidate

A dash indicates genes that have not yet been implicated in ID, but fulfil the criteria for diagnostic reporting of a pathogenic variant (that is, a possible cause for ID).

<sup>†</sup> Predicted effect on splicing.

<sup>‡</sup> PhyloP score for nonsense and frameshift mutations is not provided as this are deleterious mutations regardless of their evolutionary conservation.

<sup>§</sup> 'Known' refers to known ID gene whereas 'Candidate' refers to a gene that is listed on the candidate ID gene list.

<sup>||</sup> Since the inclusion of this patient in this study, the same *de novo* mutation in *ALG13* has been described elsewhere<sup>16</sup>. This may suggest that this mutation, despite its low conservation and the identification of a nonsense mutation in *RAI1*, may also contribute to the disease phenotype in this patient. See also Supplementary Table 8 legend.

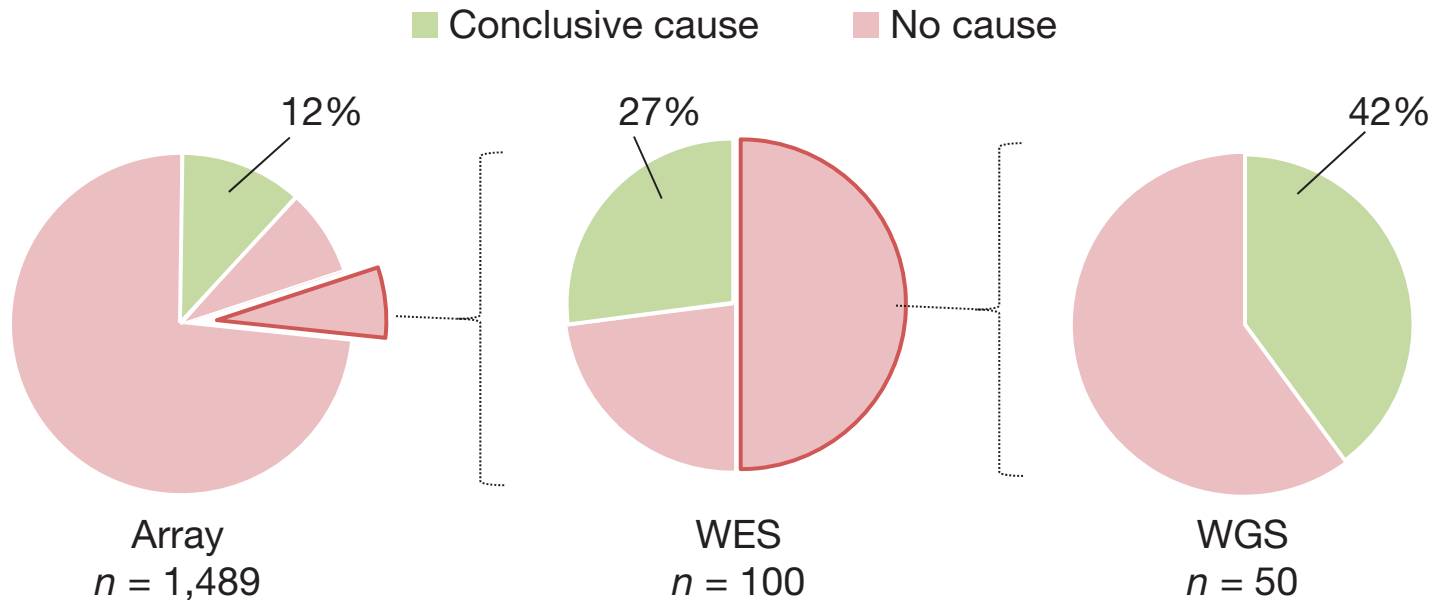


**Figure 1 | Study design and diagnostic yield in patients with severe ID per technology.** Diagnostic yield for patients with severe ID (IQ < 50), specified by technology: genomic microarrays, WES and WGS. Percentages indicate the number of patients in whom a conclusive cause was identified using the specified technique. Brackets indicate the group of patients in whom no genetic cause was identified and whose DNA was subsequently analysed using the next technology. WES data are updated with permission from ref. 6 (see Supplementary Methods).

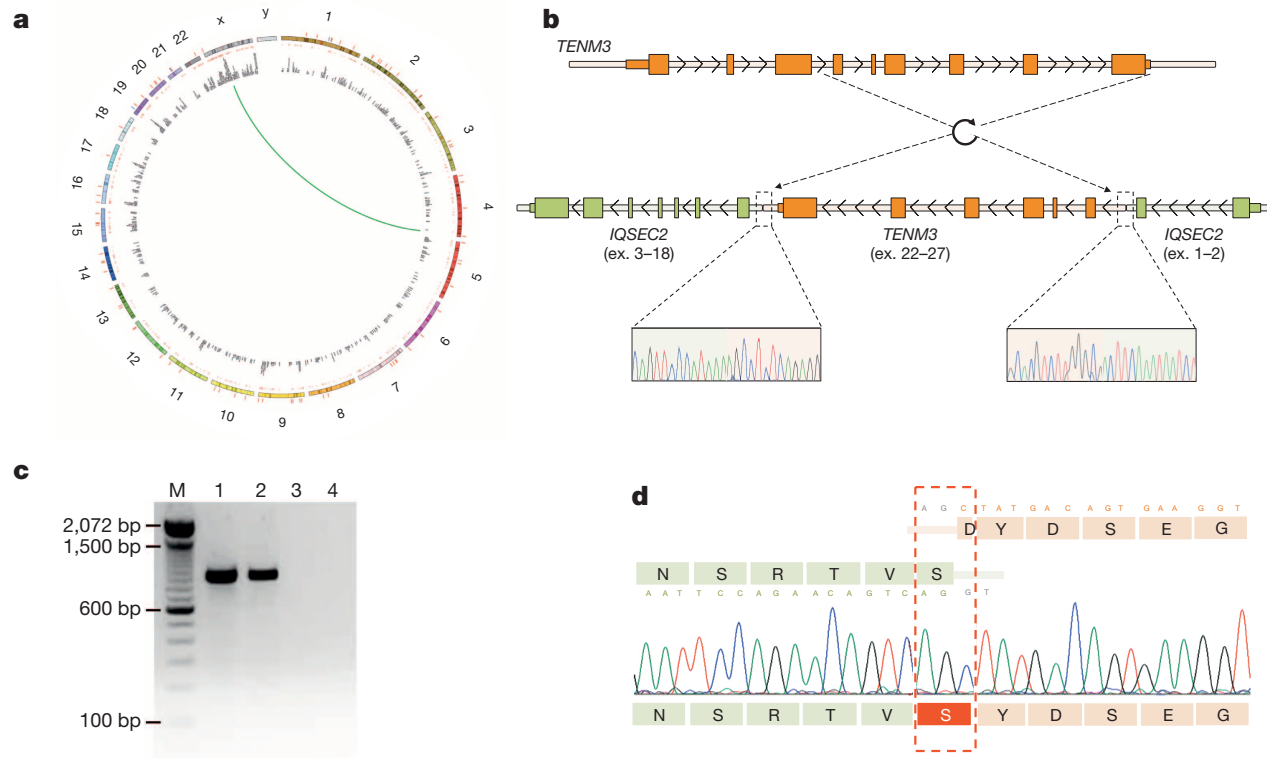


**Figure 2 | Detected duplication of a chromosome 4 region into the X-chromosomal *IQSEC2* gene.** **a–d**, Graphical representation of a *de novo* duplication–insertion event in patient 31. **a**, Circos plot with chromosome numbers and *de novo* mutations in the outer shell. Red bars represent genome-wide potential *de novo* SNVs, whereas blue lines represent potential *de novo* CNVs/structural variants. Inner shell represents the location of known ID genes (red marks) with the respective gene names. Green line illustrates a duplication event on chromosome 4, which is inserted into chromosome X. **b**, Details for inserted duplication event on chromosome X. The last six exons of

*TENM3* are inserted in inverted orientation into intron 2 of *IQSEC2*, predicted to result in an in-frame *IQSEC2-TENM3* fusion gene. ex., exon. **c**, **d**, PCR (**c**) on and Sanger sequencing (**d**) of complementary DNA junction fragment in patient 31. Lanes in **c** represent the following: M, 100 bp marker; 1, cDNA of patient with cyclohexamide treatment; 2, cDNA of patient without cyclohexamide treatment; 3, control cDNA with cyclohexamide treatment; 4, control cDNA without cyclohexamide treatment. Our data verify the presence of a fusion gene in patient 31 that is suggested to escape nonsense-mediated decay.

**Table 1 | Diagnostic yield by WGS for a pre-screened cohort of 50 ID trios**

Genetic cause	Number of patients
Total positive diagnosis	21
Dominant <i>de novo</i>	20
Autosomal SNV	11
Autosomal CNV	5
X-linked SNV	2
X-linked CNV	2
Recessive	1
Homozygous	0
Compound heterozygous	1
X-linked	0
Candidate ID genes	8
No diagnosis	21

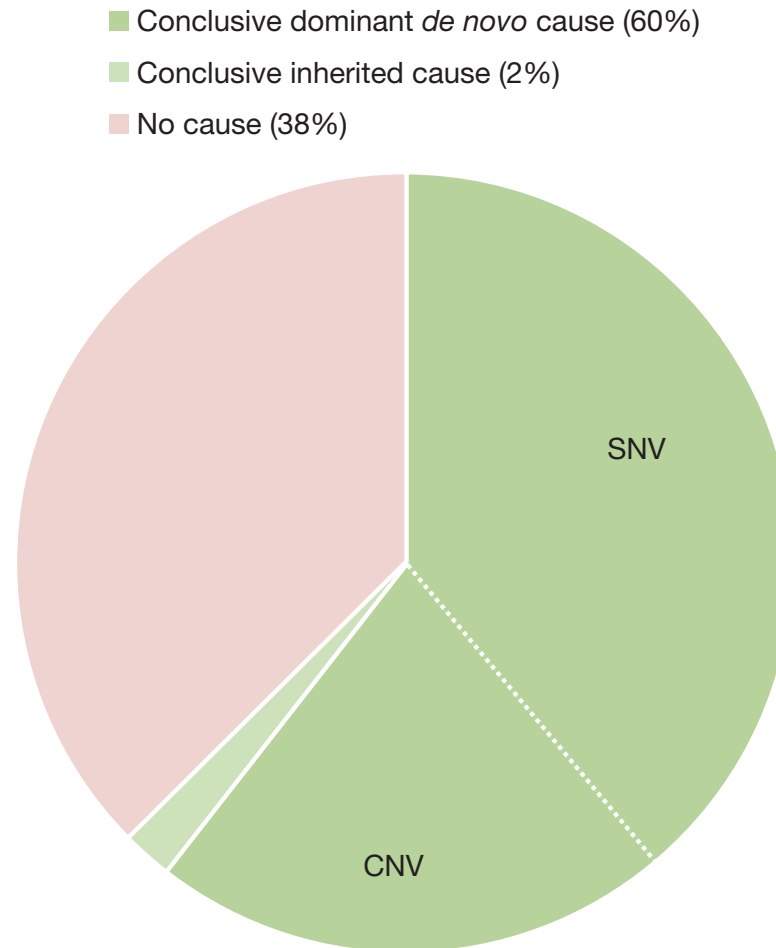


**Figure 3 | Pie chart showing role of *de novo* mutations in severe ID.** Contribution of genetic causes to severe ID on the basis of the cumulative estimates provided per technology. Our data indicate that *de novo* mutations are a major cause of severe ID. Note, small variants include SNVs and insertion/deletion events whereas large variants include structural variants and CNVs (>500 bp).

## METHODS SUMMARY

Patients were selected to have severe ID ( $IQ < 50$ ) and negative results on diagnostic genomic microarrays and exome sequencing<sup>6</sup> (Fig. 1). WGS was performed by Complete Genomics as previously described<sup>8,29</sup>. *De novo* SNVs were identified using Complete Genomics' cgatools 'calldiff' program. CNVs and structural variants were reported by Complete Genomics on the basis of read-depth deviations and discordant read pairs, respectively. *De novo* CNVs and structural variants were then identified by excluding variants with minimal evidence or overlapping with CNVs and structural variants identified in the parents or control data sets. All variants were annotated using an in-house analysis pipeline and subsequently prioritized for validation based on their confidence level (low/medium/high) and location in the genome (coding/non-coding). High-confidence candidate *de novo* mutations in non-coding variants in known ID genes were prioritized on the basis of evolutionary conservation and overlap with ENCODE chromatin state segments and transcription-factor-binding sites<sup>23</sup>. Statistical overrepresentation of mutations in known and candidate ID gene lists was calculated using Fisher's exact test based on RefSeq genes. Enrichments for loss-of-function CNV events were calculated using the exact Poisson test. To clinically interpret (*de novo*) mutations, each variant (both CNV and SNV) was assessed for mutation impact as well as functional relevance to ID according to diagnostic protocols for variant interpretation<sup>6,24–27</sup>. The diagnostic yield of WGS in an unbiased cohort was calculated based on cumulative estimates of diagnostic yield per technology (genomic microarray, WES and WGS).



## METHODS

**Patient selection.** Patients were selected to have severe ID (IQ < 50) and negative results on diagnostic genomic microarrays and exome sequencing<sup>6</sup> (Fig. 1 and Supplementary Methods).

**Whole genome sequencing.** WGS was performed by Complete Genomics as previously described<sup>8</sup>. Sequence reads were mapped to the reference genome (GRCh37) and variants were called by local *de novo* assembly according to the methods previously described<sup>29</sup>.

**Identification of *de novo* small variants.** *De novo* SNVs were identified using Complete Genomics' cgatools 'calldiff' program. On the basis of the rank order of the two confidence scores of a *de novo* mutation, we binned the variants in three groups: low confidence (at least one score < 0), medium confidence (both scores  $\geq 0$  but at least one < 5) and high confidence (both scores  $\geq 5$ ) (Supplementary Methods).

**Identification of X-linked, recessive and compound heterozygous SNVs.** Maternally inherited X-linked variants (in male patients), homozygous variants and compound heterozygous variant pairs were identified using the Complete Genomics' cgatools 'listvariants' and 'testvariants' programs to select variants according to their respective segregation. Compound heterozygous variants affecting the same gene were identified using RefSeq gene annotation (Supplementary Methods).

**Identification of *de novo* CNVs and structural variants.** CNVs were reported by Complete Genomics on the basis of read-depth deviations across 2 kb windows. Structural variants were reported by Complete Genomics based on discordant read pairs. *De novo* CNVs/structural variants were then identified by excluding variants with minimal evidence or overlapping with CNVs/structural variants identified in the parents or control data sets (Supplementary Methods).

**Generation of lists for known and candidate ID genes.** To prioritize and for subsequent interpretation of *de novo* variants for each patient individually, two gene lists were generated, one containing known ID genes (defined by five or more patients with ID having a mutation in the respective gene) and one containing candidate ID genes (defined by at least one but less than five patients with ID (or a related phenotype) showing a mutation in the respective gene) (Supplementary Methods).

**Prioritization of clinically relevant SNVs and CNVs or structural variants.** All SNVs were annotated using an in-house analysis pipeline. Variants were prioritized

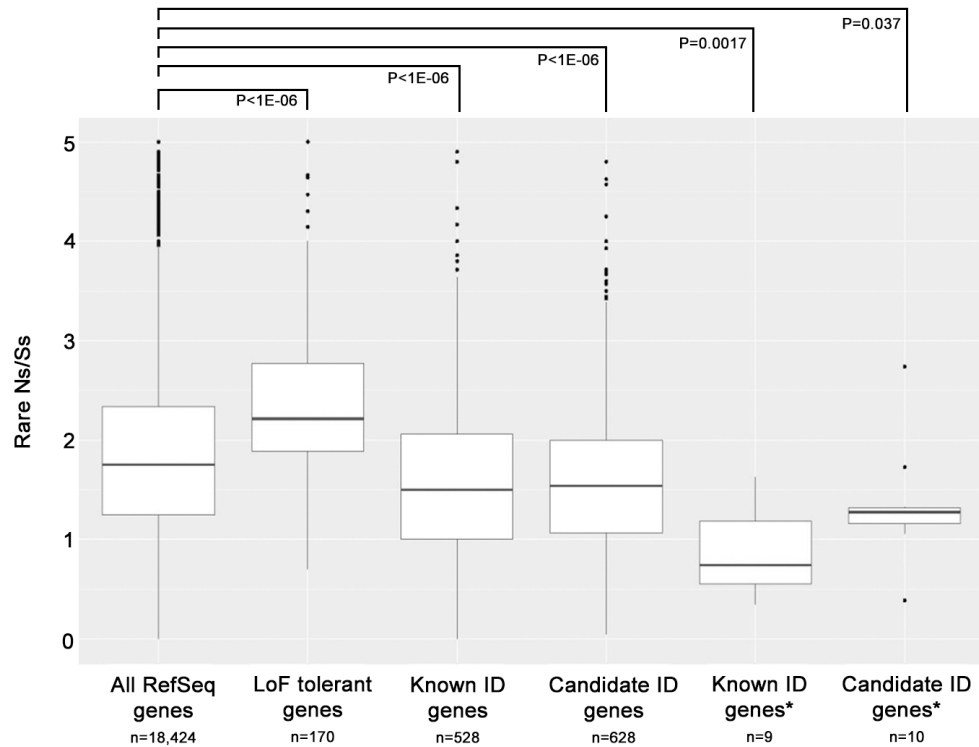
for validation in two distinct ways: (1) medium and high-confidence *de novo* SNVs and *de novo* CNVs/structural variants affecting coding regions and/or canonical splice sites; and (2) all potential *de novo* variants within known ID genes, irrespective of confidence level. Interpretation of coding *de novo* variants was performed as described previously<sup>6</sup>. High-confidence candidate *de novo* mutations in non-coding variants were prioritized on the basis of evolutionary conservation and overlap with ENCODE chromatin state segments and transcription-factor-binding sites (Supplementary Methods)<sup>23</sup>.

**Clinical interpretation of mutations.** To clinically interpret (*de novo*) mutations, each *de novo* mutation (both CNV and SNV) was assessed for mutation impact as well as functional relevance to ID according to diagnostic protocols for variant interpretation<sup>24–27</sup> that are used in our accredited diagnostic laboratory for genetic analysis (accredited to the 'CCKL Code of Practice', which is based on EN/ISO 15189 (2003), registration numbers R114/R115, accreditation numbers 095/103) (Supplementary Methods).

**Statistical analysis.** Overrepresentation of mutations in gene lists was calculated using Fisher's exact test based on the total coding size of all RefSeq genes and coding size of the genes from the respective gene list. Overrepresentation of loss-of-function mutations was calculated using Fisher's exact test based on published control cohorts. Enrichments for loss-of-function CNV events were calculated using the exact Poisson test. Enrichment for known ID genes was calculated using Fisher's exact test and odds ratios were calculated to compare the frequency of exonic CNVs in ID and control cohorts, respectively (Supplementary Methods).

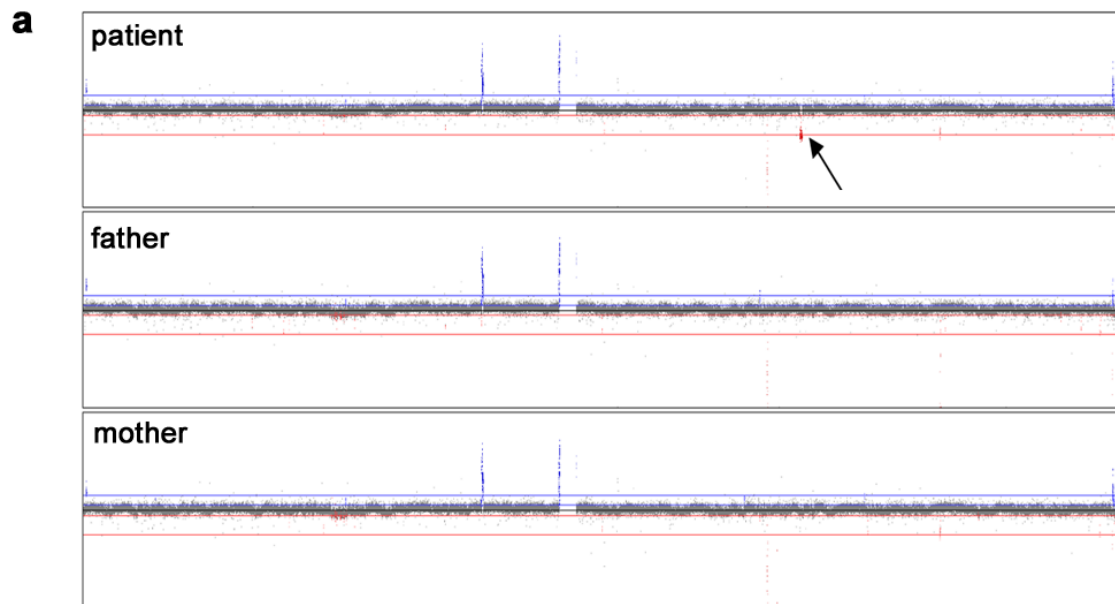
**Calculation of diagnostic yield.** Our in-house phenotypic database contains 1,489 patients with severe ID who have all had a diagnostic genomic microarray in the time period 2003–2013. In 173 (11.6%) of these patients, a *de novo* CNV was identified as a cause of ID. Subsequently, 100 array-negative patients were subjected to WES, which resulted in a *de novo* cause for ID in 27% of patients. Of all WES-negative patients, 50 were selected for this WGS study, in which 42% obtained a conclusive genetic cause. Cumulative estimates were subsequently determined using the diagnostic yield per technology (Supplementary Methods).

29. Carnevali, P. *et al.* Computational techniques for human genome resequencing using mated gapped reads. *J. Comput. Biol.* **19**, 279–292 (2012).
30. MacArthur, D. G. *et al.* A systematic survey of loss-of-function variants in human protein-coding genes. *Science* **335**, 823–828 (2012).



**Extended Data Figure 1 | Boxplots of rare missense burden in different gene sets.** Boxplots showing the difference in tolerance for rare missense variation in the general population. The vertical axis shows the distribution for each gene set of the number of rare (<1% in NHLBI Exome Sequencing Project) missense variants divided by the number of rare synonymous variants. From left to right the following gene sets are depicted: all 18,424 RefSeq genes,

170 loss-of-function tolerant genes from ref. 30, all 528 known ID genes (Supplementary Table 10), all 628 candidate ID genes (Supplementary Table 11), 9 known ID genes in which *de novo* mutations were identified in this study (Supplementary Table 8), and 10 candidate ID genes in which *de novo* mutations were identified in this study (Supplementary Table 8).

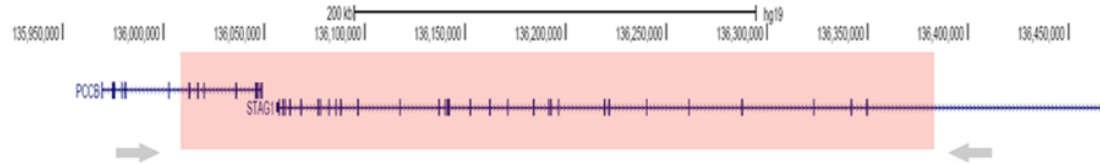


**Extended Data Figure 2 | Structural variant involving *STAG1* (patient 40).**

**a–c**, CNV identified using WGS in patient 40, including the *STAG1* gene.

**a**, Chromosome 3 profile ( $\log_2$  test over reference (T/R) ratios) based on read-depth information for patient, father and mother. Black arrow points

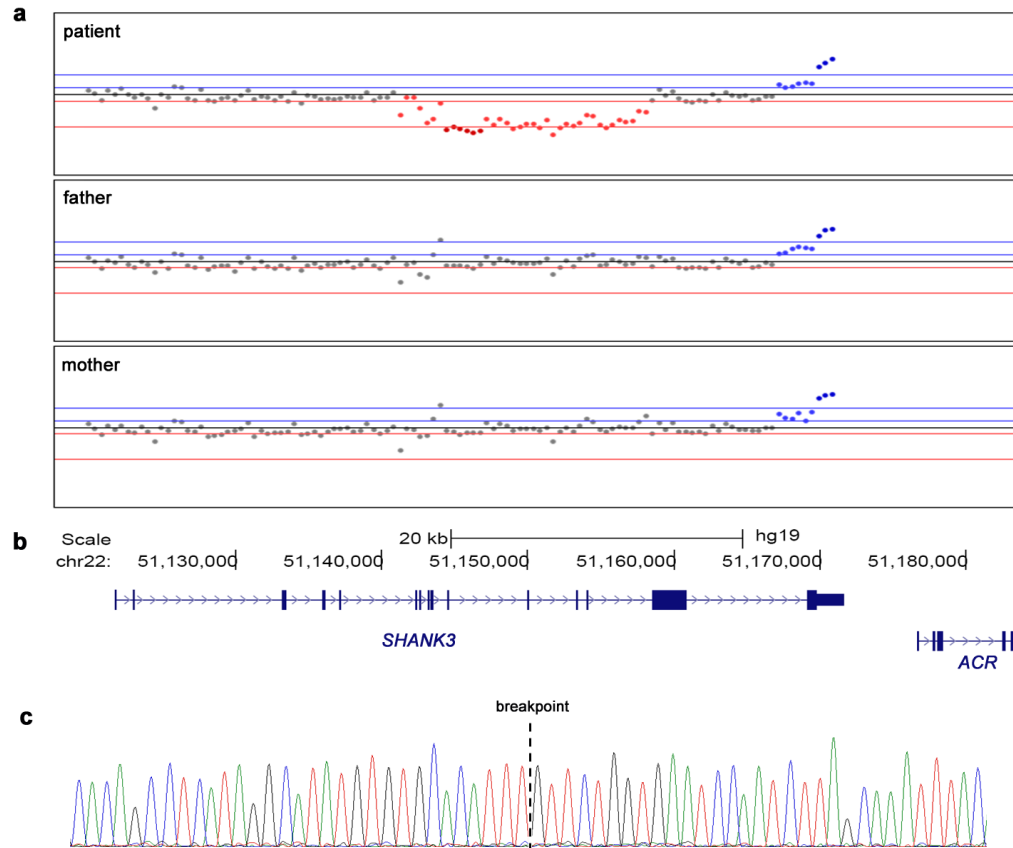
towards the *de novo* event in patient 40. **b**, Genic contents of deletion. Grey arrows show primers used to amplify the junction fragment. **c**, Details on the proximal and distal breakpoints, showing the ‘fragmented’ sequence at both ends. Breakpoints are provided in Extended Data Table 1.

**b****c**

tgcagttcct tacctgcaat aaaaataatt cctgaccag atctaggttg  
 ttacctgcat tctcattggc tttcagcata gtgatgataa ggtgtaaatg  
 GAGAGAGGGT TTTGGCATGA AATCTGTAGC TTGTGGGGGT TCAGTGGCAG  
 GGGATGCTTA TGTACTTCAT TGGTGGGTGA TTTTACTTGT TGATCTGABT T deleted  
 TGCAAAATGAT TTTCAGGTAA TCAAAGAATC CTGTCCTTTG ACCAGATAGA  
 TGAAGTCTTA CTGAGTCCTA TTCAAGAAGT TTCTGAGGGA AGGCTTTTCT  
 GTAATCTGTT TATTGGGAAG TTGTTTCT CTTTATTCT TCAGCTCCTT  
 GCCATTTTAT TACATTGTGT CCATAATGGT AAAGGATTA TCTGATCTCA  
 CACTTCATT TCAGAGGTAC ATATCTTTAT TACATGACTT TAATGACTT  
 ATATTTTAAA AATATTTTAA AATGAAGTCT ATTTGAAGTT ATACATGAGT  
 AATTACCATT CATCTCAAAC CTGCTTTAA Aaaaatcagc cttttcttct  
 taaaaatatta ataaaaatga acattggatg ccaagacaga atggttgggg  
 ggaaaaaagta gtgatagcca tccaacttga ggagaggagt tctagaggga  
  
 ggttgatca cctgaggtca ggagttcaag accagcctgg ccaacatggc  
 gaaaccccat ctctactaaa aatacaaaaa aattagcaag gcatggtggt  
 gggcacctgt aatcccagct actcaggaga ctgaggtagg agaatcgcta  
 gaacccctga ggtggaggtt gcagtGAGCC GAGATCACGC CATTGCACTC  
 CAGCCTGGGT GACAGAGTGA aactctgtct ttaaaaaaa aaaaaaaac Deleted  
 ctgtttATG CTAGGATTCA ACTCCAAGTA GTGTGGCTTG TGCTCTTAAA  
 TGAAGAGAT AATATAAGCA ACAAGGAACA GAGACAGCTG AGCATCTAGA  
 AAGAAACTG AACCTGGCAA AGCTGAGATA CATGGAATTA TATTCCACCT  
 ATATAGTTTC AACCAAACCA CTCACTTCTG GACTAAGTTA TATTATGTA Deleted  
 ATTATAGCAA ATAAATTAC TGATTTTCAA TTTTAAAAT CAATtttac  
 tcaataggcg gtctaataa tatatacaac taagtataa cataagcttt  
 aacaaggtaa aaataacatc accagtaaac aaaaatttaa aaatg

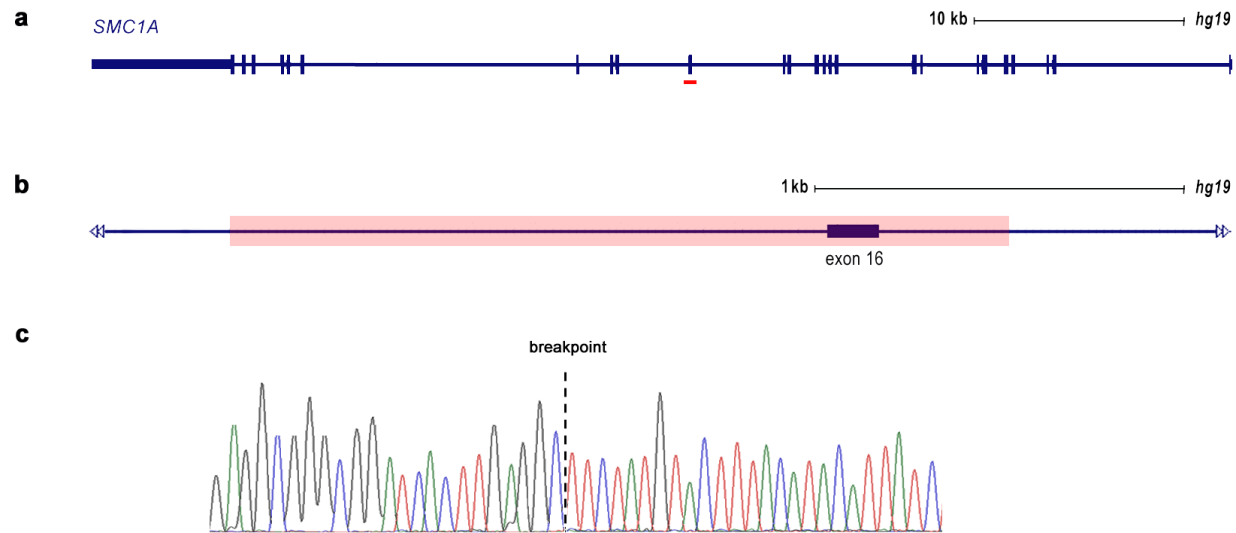
**Extended Data Figure 2 | Structural variant involving *STAG1* (patient 40).**  
**a–c,** CNV identified using WGS in patient 40, including the *STAG1* gene.  
**a,** Chromosome 3 profile ( $\log_2$  test over reference (T/R) ratios) based on read-depth information for patient, father and mother. Black arrow points

towards the *de novo* event in patient 40. **b,** Genic contents of deletion. Grey arrows show primers used to amplify the junction fragment. **c,** Details on the proximal and distal breakpoints, showing the ‘fragmented’ sequence at both ends. Breakpoints are provided in Extended Data Table 1.



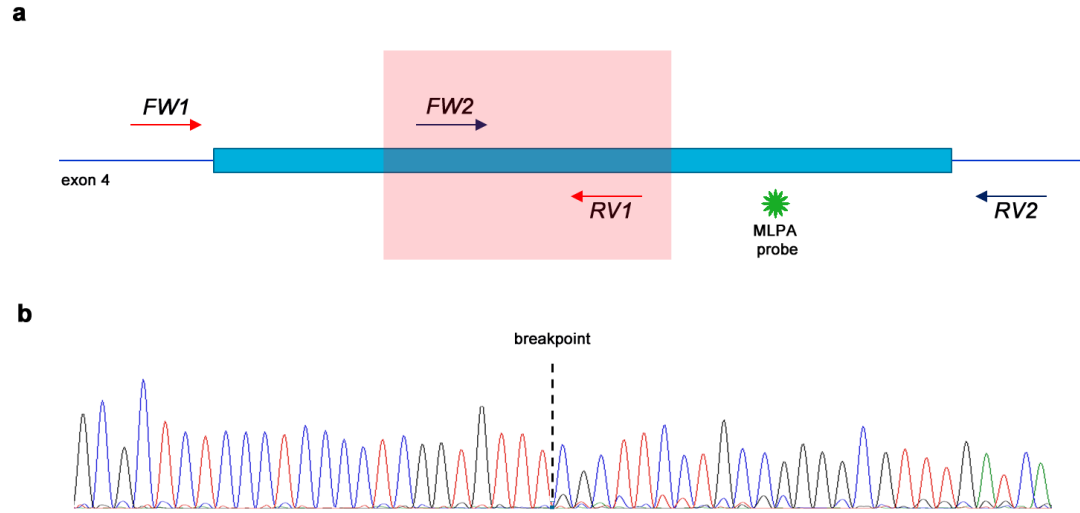
**Extended Data Figure 3 | Structural variant involving *SHANK3* (patient 5).**  
**a–c**, CNV identified using WGS in patient 5, including the *SHANK3* gene.  
**a**, Detail of chromosome 22 profile ( $\log_2$  T/R ratios) based on read-depth information for patient, father and mother. Red dots in top panel show ratios indicating the *de novo* deletion in patient 5. **b**, Genic content of the deletion.

**c**, Sanger validation for the junction fragment. Dotted vertical line indicates the breakpoint with sequence on the left side originating from sequence proximal to *SHANK3* and on the right side sequence that originates from sequence distal to *ACR*. Breakpoints are provided in Extended Data Table 1.



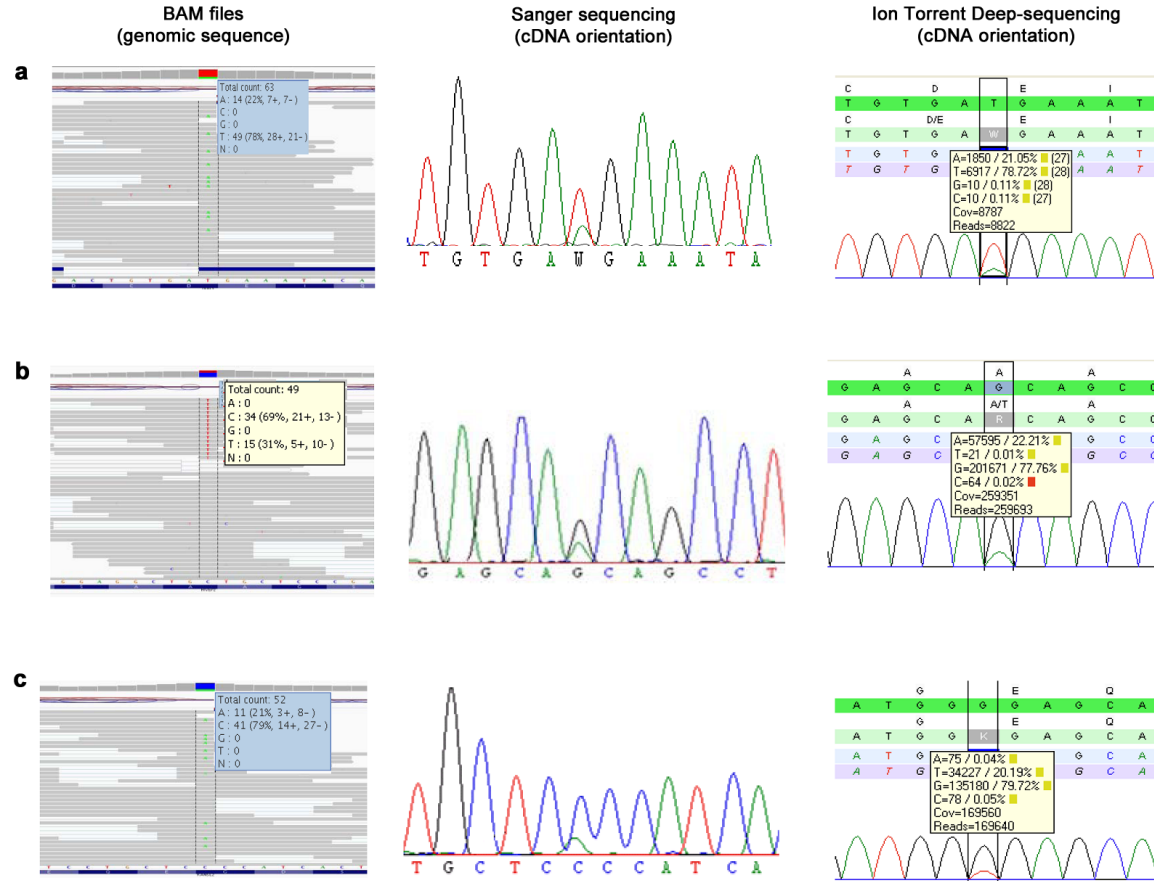
**Extended Data Figure 4 | Single-exon deletion involving *SMC1A* (patient 48).** **a**, Schematic depiction of the deletion identified in patient 48 involving a single exon of *SMC1A*. Pink horizontal bar highlights the exon that was deleted in the patient. **b**, Details at the genomic level of the deletion including

exon 16, with Sanger sequence validation of the breakpoints. Junction is indicated by a black vertical dotted line. Breakpoints are provided in Extended Data Table 1.



**Extended Data Figure 5 | Intra-exonic deletion involving *MECP2* (patient 18).** **a**, Schematic depiction of the deletion identified in patient 18, which is located within exon 4 of *MECP2*. Initial Sanger sequencing in a diagnostic setting could not validate the deletion as the primers used to amplify exon 4 removed the primer-binding sites (FW2 and RV1 respectively). Multiplex ligation probe amplification (MLPA) analysis for CNV detection showed

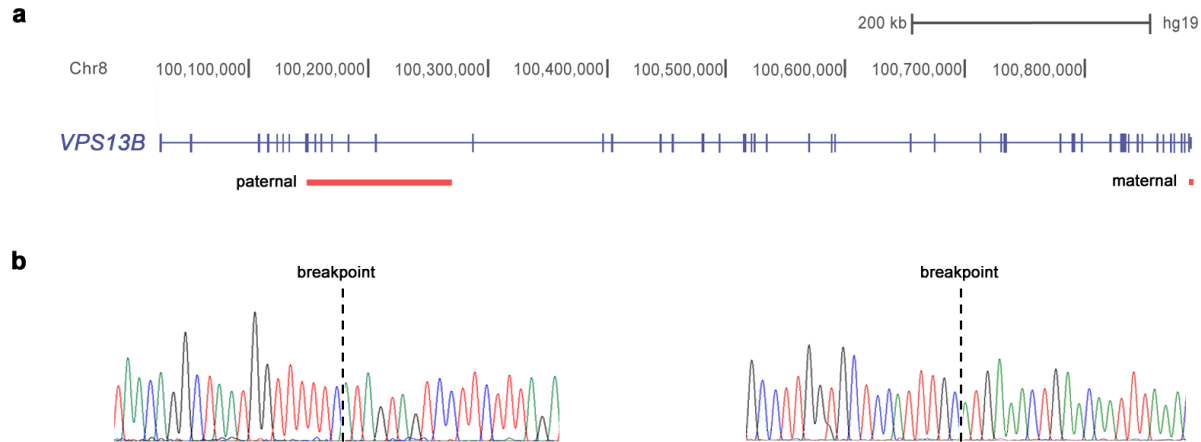
normal results as the MLPA primer-binding sites were located just outside of the deleted region. **b**, Combining primers FW1 and RV2 amplified the junction fragment, clearly showing the deletion within exon 4. Of note, the background underneath the Sanger sequence is derived from the wild-type allele. Breakpoints are provided in Extended Data Table 1.



**Extended Data Figure 6 | Confirmation of mosaic mutations in *PIAS1*, *HIVEP2* and *KANSL2*.** a–c, Approaches used to confirm the presence of mosaic mutations in *PIAS1* (a), *HIVEP2* (b) and *KANSL2* (c). Images and read-depth information showing the base counts in the BAM files (left) indicated that the variants/wild-type allele were not in a 50%/50% distribution. Sanger sequencing (middle) then confirmed the variant to be present in the patient,

and absent in the parents (data from parents not shown), again indicating that the mutation allele is underrepresented. Guided by these two observations, amplicon-based deep sequencing using Ion Torrent subsequently confirmed the mosaic state of the mutations (right). On the basis of deep sequencing, percentages of mosaicism for *PIAS1*, *HIVEP2* and *KANSL2* were estimated at 21%, 22% and 20%, respectively.





**Extended Data Figure 7 | Compound heterozygous structural variation affecting *VPS13B* (patient 12).** **a, b,** CNVs of *VPS13B* identified using WGS in patient 12. **a,** Schematic representation of *VPS13B*, with vertical bars indicating coding exons. In patient 12 two deletions were identified, one ~122 kb in size which was inherited from his father, and another ~2 kb in size, which was

inherited from his mother and consisted only of a single exon. **b,** Both CNV junction fragments were subsequently validated using Sanger sequencing. Left, junction fragment from the paternally inherited deletion. Right, junction fragment from the maternally inherited deletion. Breakpoints are provided in Extended Data Table 1.

**Extended Data Table 1 | Large variants of potential clinical relevance identified using WGS and probability of exonic CNVs occurring in affected and control individuals for these loci**

Trio	Type*	Genomic characterization	Size (kb)	CN	Origin	Genes affected	Affected (n=7,743)	Controls (n=4,056)	OR	CI	P-value <sup>#</sup>
5	CNV	chr22(GRCh37):g.51121756-51187704del	66	1	<i>De novo</i>	<b>SHANK3</b> ; <i>ACR</i>	41	4	5.4	1.9-15.0	0.0013
18	SV	chrX(GRCh37):g.153295929-153296514del	0.6	1	<i>De novo</i>	<b>MECP2</b> <sup>§</sup>	41	0	22.6	1.4-367.6	0.04
31	CNV complex	chr4(GRCh37):g.183693432-183756173dup	62	3	<i>De novo</i>	<i>TENM3</i>	5	0	0.6	0.2-2.4	1.0
		Insertion point: chrX(GRCh37):g.53318362-53318363	-	-		<b>IQSEC2</b>	28	0	7.6	1.0-56.1	0.092
37	CNV complex	chr3(GRCh37):g.48532000-49156000dup <sup>†</sup>	624	3	<i>De novo</i>	n=22 <sup>  </sup>	22	0	23.6	1.4-388.7	0.033
		chr3(GRCh37):g.49298000-49848000dup <sup>†</sup>	550	3		n=20 <sup>  </sup>					
		chr3(GRCh37):g.49849505-49870969del	21	1		n=2 <sup>  </sup>					
		chr3(GRCh37):g.49872000-49958000dup <sup>†</sup>	86	3		n=4 <sup>  </sup>					
40	CNV	chr3(GRCh37):g.136003159delinsGATGTTTCA	-								
		chr3(GRCh37):g.136003363-136385607del	382	1	<i>De novo</i>	<b>STAG1</b> ; <i>PCCB</i>	9 <sup>¶</sup>	0	10.0	0.6-171.1	0.26
		chr3(GRCh37):g.136385640-136385685del	-								
		chr3(GRCh37):g.136385737-136385739del	-								
48	SV	chrX(GRCh37):g.53424894-53427008del	2.1	1	<i>De novo</i>	<b>SMC1A</b> <sup>§</sup>	33	0	17.3	1.1-282.9	0.075
49	SV	chr1(GRCh37):g.40247181-40256104dup	9	3	<i>De novo</i>	<b>BMP8B</b> <sup>§</sup>	2	0	2.6	0.1-54.6	1.0
50	CNV	chr16(GRCh37):g.29567295-30177916 <sup>‡</sup>	611	1	<i>De novo</i>	n=29 <sup>  </sup>	31	4	4.1	1.4-11.5	0.0093
12	SV	chr8(GRCh37):g.100887349-100889133del	1.7	1	<i>Maternal</i>	<b>VPS13B</b> <sup>§,☆</sup>	5	0	5.8	0.3-104.2	0.80
	CNV	chr8(GRCh37):g.100147792-100270123del	122	1	<i>Paternal</i>	<b>VPS13B</b> <sup>‡</sup>	0	0			

Genes highlighted in bold are either listed as known ID genes or candidate ID genes. Please note that all patients had 250K SNP microarrays. Re-evaluation of these data showed that for all but one CNV the number of probes within the region was insufficient, either because of the small genomic size of the CNV, or due to uneven genome-wide probe spacing leaving fewer probes than required for the hidden Markov model algorithms to be identified.

\* Primary method used to identify the rearrangement (see also Supplementary Methods).

† Not assessed at base-pair level due to complexity of CNV event including an inversion, duplication and deletion.

‡ Not assessed at base-pair level as the CNV event, involving a known microdeletion syndrome region, is mediated by low-copy repeats.

§ Single exon.

|| Number of genes affected rather than individual gene names are provided due to the large number of genes.

¶ Observed 13 times in Decipher.

# Corrected for multiple testing using Benjamini–Hochberg with a false discovery rate (FDR) of 0.1.

☆ *VPS13B* recessive ID gene.

**Table 1: Re-evaluated molecular diagnosis in 100 patients with severe ID after publication of diagnostic exome sequencing in patients with severe ID.**

Patient ID in de Ligt et al	Molecular diagnosis	Based on [gene] (inheritance)	Re-evaluated molecular diagnosis	Based on [gene] (inheritance)	Change due to:
4	Highly likely	<i>PDHA1</i> (X-linked)	NO	-	X-linked variant does not segregate
5	Possibly	<i>PHIP</i> (de novo)	Highly likely	<i>PHIP</i> (de novo)	In house 2nd case identified through diagnostic WES in patient with severe ID
6	Possibly	<i>PSMA7</i> (de novo)	Highly likely	<i>EHMT1</i> deletion (de novo)	CNV calling on WES data identified deletion of <i>EHMT1</i> (de novo)
14	NO		Highly likely	<i>DDX3X</i> (de novo)	Bioinformatic re-analysis of WES data identified de novo mutation in <i>DDX3X</i> ; A second patient was subsequently identified by diagnostic WES in a patient with ID
18	Highly likely	<i>ARHGEF9</i> (X-linked)	NO		X-linked variant does not segregate
40	Possibly	<i>WAC/ MIB1</i> (de novo)	Highly likely	<i>WAC</i> (de novo)	In house 2nd case identified through diagnostic WES in patient with severe ID
60	NO		Highly likely	<i>TCF4</i> (de novo)	Bioinformatic re-analysis identified a de novo mutation in <i>TCF4</i>
72	Possibly	<i>PPP2R5D</i> (de novo)	Highly likely	<i>PPP2R5D</i> (de novo)	2nd case identified in house in patient with severe ID
74	Possibly	<i>KIF5C</i> (de novo)	Highly likely	<i>KIF5C</i> (de novo)	Literature reports additional patient with de novo mutation in <i>KIF5C</i>
77	NO		Highly likely	<i>STXBP1</i> (de novo)	Bioinformatic re-analysis identified a de novo mutation <i>STXBP1</i>
85	NO		Highly likely	<i>SCN2A</i> (de novo)	Bioinformatic re-analysis identified a de novo mutation in <i>SCN2A</i>
87	Possibly	<i>RAPGEF1</i> (de novo)	Highly likely	<i>MECP2</i> (de novo)	Bioinformatic re-analysis identified <i>MECP2</i> de novo mutation
91	Possibly	<i>EEF1A2</i> (de novo)	Highly likely	<i>EEF1A2</i> (de novo)	2nd patient in literature with exact same de novo mutation
92	Possibly	<i>MYT1L</i> (de novo)	Highly likely	<i>MYT1L</i> (de novo)	Overlapping small CNV containing <i>MYT1L</i> described in literature
96	NO		Highly likely	<i>ADNP</i> (de novo)	Bioinformatic re-analysis of WES data identified a de novo

**Table 2: Cross-references for patient numbers used in de Ligt et al. and the current study**

Trio ID current study	Trio ID de Ligt et al. 2012
<b>1</b>	1
<b>2</b>	4
<b>3</b>	8
<b>4</b>	10
<b>5</b>	12
<b>6</b>	17
<b>7</b>	18
<b>8</b>	19
<b>9</b>	20
<b>10</b>	21
<b>11</b>	23
<b>12</b>	24
<b>13</b>	26
<b>14</b>	27
<b>15</b>	28
<b>16</b>	30
<b>17</b>	33
<b>18</b>	34
<b>19</b>	35
<b>20</b>	36

Trio ID current study	Trio ID de Ligt et al. 2012
<b>21</b>	37
<b>22</b>	38
<b>23</b>	44
<b>24</b>	45
<b>25</b>	46
<b>26</b>	47
<b>27</b>	49
<b>28</b>	50
<b>29</b>	51
<b>30</b>	53
<b>31</b>	55
<b>32</b>	56
<b>33</b>	57
<b>34</b>	65
<b>35</b>	67
<b>36</b>	68
<b>37</b>	71
<b>38</b>	73
<b>39</b>	75
<b>40</b>	76

Trio ID current study	Trio ID de Ligt et al. 2012
<b>41</b>	78
<b>42</b>	80
<b>43</b>	82
<b>44</b>	86
<b>45</b>	94
<b>46</b>	95
<b>47</b>	97
<b>48</b>	98
<b>49</b>	99
<b>50</b>	100

**Table 3: De novo pathogenic and non-pathogenic variants previously detected using WES used to optimize de novo variant detection**

Trio ID	Gene	Genomic position (GRCh37)	Protein level	Variant in WGS data	Identified as de novo mutation?
<i>A: Known pathogenic mutations in patients with severe ID identified using WES</i>					
<b>Pos. control 1</b>	<b>TCF4</b>	Chr18(GRCh37):g.52896230C>T	p.(Arg576Gln)	+	<i>n.a.</i>
<b>Pos. control 2</b>	<b>SCN2A</b>	Chr2(GRCh37):g.166231415G>A	p.(Trp1398*)	+	<i>n.a.</i>
<b>Pos. control 3</b>	<b>GRIN2B</b>	Chr12(GRCh37):g.13764781G>A	p.(Pro553Leu)	+	<i>n.a.</i>
<b>Pos. control 4</b>	<b>GRIN2A</b>	Chr16(GRCh37):g.9928084G>C	p.(Pro522Arg)	+	<i>n.a.</i>
<b>Pos. control 5</b>	<b>PDHA1</b>	ChrX(GRCh37):g.19369435delinsAGA	p.(Pro110Argfs*71)	+	<i>n.a.</i>
<b>Pos. control 6</b>	<b>GATAD2B</b>	Chr1(GRCh37):g.153785737G>A	p.(Gln470*)	+	<i>n.a.</i>
<b>Pos. control 7</b>	<b>CTNNB1</b>	Chr3(GRCh37):g.41275106-41275109del	p.(Ser425Thrfs*11)	+	<i>n.a.</i>
<b>Pos. control 8</b>	<b>LRP2</b>	Chr2(GRCh37):g.170009333del	p.(Gly4146Glufs*2)	+	<i>n.a.</i>
<i>B: De novo mutations identified using WES<sup>2</sup> that are not considered to be the cause of ID</i>					
<b>2</b>	<b>TRIO</b>	Chr5(GRCh37):g.14390384A>T	p.(Aps1368Val)	+	+
<b>3</b>	<b>C15orf40</b>	Chr15(GRCh37):g.83677401C>T	p.(Ala89Thr)	+	+
<b>3</b>	<b>RB1</b>	Chr13(GRCh37):g.48921977T>C	p.(Tyr173His)	+	+
<b>4</b>	<b>CNGA3</b>	Chr2(GRCh37):g.99012638G>T	p.(Trp335Cys)	+	+
<b>4</b>	<b>CXXC11</b>	Chr2(GRCh37):g.242814942G>A	p.(Gly412Asp)	+	-
<b>7</b>	<b>CLRN3</b>	Chr10(GRCh37):g.129690984A>T	p.(Ile22Asn)	+	+
<b>7</b>	<b>OSBPL9</b>	Chr1(GRCh37):g.52231512C>T	p.(Pro276Leu)	+	+
<b>10</b>	<b>MFAP3</b>	Chr5(GRCh37):g.153429439A>G	p.(Ser53Gly)	+	+
<b>13</b>	<b>FHDC1</b>	Chr4(GRCh37):g.153884006G>C	p.(Leu297Phe)	+	+
<b>21</b>	<b>ALG13</b>	ChrX(GRCh37):g.110928268A>G	p.(Asn107Ser)	+	+
<b>21</b>	<b>KRT32</b>	Chr17(GRCh37):g.39623313C>T	p.(Glu89Lys)	+	+
<b>22</b>	<b>HADHA</b>	Chr2(GRCh37):g.26457124C>T	p.(=)	+	+
<b>23</b>	<b>ZNF831</b>	Chr20(GRCh37):g.57829608G>A	p.(Arg1615His)	+	+
<b>29</b>	<b>USP8</b>	Chr15(GRCh37):g.50790871G>A	p.(=)	+	+
<b>30</b>	<b>NEK1</b>	Chr4(GRCh37):g.170359295T>G	p.(Lys901Asn)	+	-*
<b>36</b>	<b>ATP7B</b>	Chr13(GRCh37):g.52536008G>A	p.(=)	+	+
<b>39</b>	<b>EFS</b>	Chr14(GRCh37):g.23829243G>A	p.(=)	+	+
<b>40</b>	<b>ZFYVE16</b>	Chr5(GRCh37):g.79733643C>T	p.(Ala380Val)	+	+
<b>43</b>	<b>C20orf26</b>	Chr20(GRCh37):g.20243639A>C	p.(Thr790Pro)	+	+
<b>44</b>	<b>RBL2</b>	Chr16(GRCh37):g.53472982G>T	p.(Val99Phe)	+	+
<b>47</b>	<b>ABCC8</b>	Chr11(GRCh37):g.17483205G>A	p.(=)	+	+

+: Identified; -: not identified; *n.a.*: not assessed. \*Variant was detected as somatic variant in the patient after deep-sequencing (see also Figure 1). Trio ID refer to numbers used in this study.

***Table 4: Classification of genes according to the frequency of reported pathogenic mutations***

	Total genes	Known ID gene	Candidate ID gene
HGMD with phenotype ID or MR	368	347	21
PubMed search 'WES+ID'	154	102	52
Diagnostic gene list	494	407	87
Large-scale sequencing studies with overlapping phenotypes	462	77	385
<b>Total unique genes</b>		<b>528</b>	<b>628</b>

**Table 5: Overview of de novo mutations in healthy individuals**

	Number of controls (c) or siblings (s)	Total	LoF	Missense	Synonymous
Rauch <i>et al.</i>	20 (c)	24	2	15	7
O'Roak <i>et al.</i>	50 (s)	29	1	19	9
Sanders <i>et al.</i> *	200 (s)	125	5	82	38
Iossifov <i>et al.</i> **	343 (s)	288	12	203	73
Gulsuner <i>et al.</i>	84 (c)	67	12	36	19
Xu <i>et al.</i> ***	34 (c)	16	0	11	5
<b>Total</b>	<b>731</b>	<b>549</b>	<b>32</b>	<b>366</b>	<b>151</b>

*Putative LoF includes nonsense, frameshift and canonical splice site mutations based on gene annotation; \* study did not consider indels; \*\* not all de novo mutations were validated by Sanger sequencing; \*\*\*excluded splice site variants if not in canonical di-nucleotide of splice site. For some studies the numbers deviate from the numbers given in the main publication, numbers considered here were retrieved from de novo mutation overviews from supplementary tables.*

**Table 6: De novo mutations in dominant ID genes in control individuals**

chr	genomic position	Mutation type	Ref	Mut	Gene	Protein change	PhyloP	known or candidate ID gene
chr12	51090925	Missense	C	T	<i>DIP2B</i>	p.Thr672Met	4.27	candidate
chr17	29684348	Missense	C	T	<i>NF1</i>	p.Ala2623Val	5.50	known
chr5	176715871	Missense	C	G	<i>NSD1</i>	p.Thr2068Ser	6.08	known
chr10	123260408	Missense	G	A	<i>FGFR2</i>	p.Ala498Val	6.22	known
chr17	17697260	inframe insertion	-	AGT	<i>RAI1</i>	p.Gln333_Tyr334insVal	-	known
chr12	13716876	frameshift	CG	N	<i>GRIN2B</i>	p.Arg1099fs	-	known



**Table 7: Calculation of de novo mutations as cause of severe ID**

	Diagnostic yield in cohort	Estimated cumulative percentage
<b>Genomic microarray</b> <b>(n=1,489 patients with severe ID)</b>		
<i>De novo dominant cause by CNV (n=173)</i>	11.60%	11.60%
<b>Whole Exome Sequencing</b> <b>(n=100 array negative patients)</b>		
<i>De novo dominant cause by SNV (n=25)</i>	25.00%	22.10%
<i>De novo dominant cause by CNV (n=1)</i>	1.00%	0.88%
<i>Recessive cause by SNV (n=1)</i>	1.00%	0.88%
<b>Whole Genome Sequencing</b> <b>(n=50 WES negative patients)</b>		
<i>De novo dominant cause by SNV (n=13)</i>	26.00%	16.77%
<i>De novo dominant cause by CNV (n=7)</i>	14.00%	8.39%
<i>Recessive cause by SNV (n=1)</i>	2.00%	1.29%

**Supplementary Table 2: Average genome sequencing statistics per individual**

Genome	Average
<b>Fully called genome fraction</b>	<b>0.98</b>
<i>No-called called genome fraction</i>	<i>0.02</i>
<i>Reference genome fraction of bases with coverage &gt;= 40x</i>	<i>0.92</i>
<b>Total number of called single nucleotide substitution variants</b>	<b>3,509,927</b>
<b>Total number of called insertion variants</b>	<b>384,487</b>
<b>Total number of called deletion variants</b>	<b>375,832</b>
<b>Total number of complex single nucleotide variants</b>	<b>176,009</b>
<b>Total CNV segment count</b>	<b>276</b>

Exome*	Average
<b>Fully called exome fraction</b>	<b>0.99</b>
<i>No-called exome fraction</i>	<i>0.01</i>
<i>Exome fraction of bases with coverage &gt;= 40x</i>	<i>0.94</i>
<b>Total number of single nucleotide substitution variants</b>	<b>22,186</b>
Synonymous SNV loci	10,744
Non-synonymous SNV loci	10,081
<i>Missense</i>	<i>9,966</i>
<i>Nonsense</i>	<i>84</i>
<i>Disruption stop codon</i>	<i>12</i>
<i>Disruption initiation codon</i>	<i>20</i>
<i>Block substitutions</i>	<i>77</i>
<b>Total number of insertion variants</b>	<b>590</b>
<b>Total number of deletion variants</b>	<b>484</b>
<b>Total number of complex single nucleotide variants</b>	<b>1,243</b>

Sequencing statistics as supplied by Complete Genomics. Genome fractions are based on the GRCh37 reference genome. Number of variants represent unfiltered total calls as made by Complete Genomics. Functional annotation of SNVs is based on RefSeq annotation by Complete Genomics. \*'Exome' as defined by Complete Genomics.

**Supplementary Table 3: Comparison of variants between WES and WGS identified in regions targeted by exome enrichment kit**

Overlap for WGS and WES	Average (150 samples)	SD
<b>Total number of variants</b>	<b>16,964</b>	<b>1,716</b>
<i>Insertions/Deletions</i>	843	110
<i>In regions with high WES coverage</i>	1,392	1,018
<i>In regions with low WES coverage</i>	1,219	319
<b>Variants in coding sequence</b>	<b>10,812</b>	<b>975</b>

Whole Genome Sequencing only	Average (150 samples)	SD
<b>Total number of variants</b>	<b>28,028</b>	<b>2,187</b>
<i>Insertions/Deletions</i>	2,579	168
<i>In regions with high WES coverage</i>	1,450	835
<i>In regions with low WES coverage</i>	10,480	1,633
<b>Variants in coding sequence</b>	<b>11,333</b>	<b>1,186</b>

Whole Exome Sequencing only	Average (150 samples)	SD
<b>Total number of variants</b>	<b>1,213</b>	<b>123</b>
<i>Insertions/Deletions</i>	94	18
<i>In regions with high WES coverage</i>	357	92
<i>In regions with low WES coverage</i>	60	18
<b>Variants in coding sequence</b>	<b>622</b>	<b>64</b>

Comparison between variants called by genome sequencing and exome sequencing within the targets of the Agilent 50Mb exome enrichment kit (v2). Variants called exclusively by genome sequencing tended to lie in regions with very low exome coverage, whereas variants called exclusively by exome sequencing tended to lie in regions of very high exome coverage. This latter is likely due to mapping issues in repeat regions. Note, regions of very high exome coverage are defined as regions of at least three times the median exome coverage. Regions of very low exome coverage are regions with less than one third of the median exome coverage.

**Supplementary Table 4: Overview of putative de novo SNVs detected through WGS**

	High confidence				Medium confidence				Low confidence			
	Sum	Min	Max	Median	Sum	Min	Max	Median	Sum	Min	Max	Median
<b>Total</b>	<b>4,081</b>	<b>47</b>	<b>111</b>	<b>82</b>	<b>5,034</b>	<b>68</b>	<b>142</b>	<b>98.5</b>	<b>62,622</b>	<b>909</b>	<b>1,500</b>	<b>1,279</b>
<b>Exonic</b>	<b>80</b>	<b>0</b>	<b>5</b>	<b>1</b>	<b>82</b>	<b>0</b>	<b>5</b>	<b>1</b>	<b>670</b>	<b>6</b>	<b>23</b>	<b>14</b>
<i>Missense</i>	51	0	1	1	49	0	0	1	360	5	0	10
<i>Synonymous</i>	21	0	2	0	21	0	2	0	189	1	10	3
<i>Nonsense</i>	8	0	2	0	3	0	1	0	20	0	3	0
<i>In-frame insertions</i>	0	0	0	0	1	0	1	0	5	0	1	0
<i>In-frame deletions</i>	0	0	0	0	1	0	1	0	8	0	1	0
<i>In-frame complex</i>	0	0	0	0	0	0	0	0	1	0	1	0
<i>Out-of-frame insertions</i>	0	0	0	0	0	0	0	0	67	0	5	1
<i>Out-of-frame deletions</i>	0	0	0	0	4	0	1	0	18	0	2	0
<i>Out-of-frame complex</i>	0	0	0	0	0	0	0	0	2	0	1	0
<b>Splice sites</b>	<b>6</b>	<b>0</b>	<b>1</b>	<b>0</b>	<b>6</b>	<b>0</b>	<b>1</b>	<b>0</b>	<b>72</b>	<b>0</b>	<b>5</b>	<b>1</b>
<i>SA canonical</i>	1	0	1	0	1	0	1	0	4	0	1	0
<i>SD canonical</i>	0	0	0	0	1	0	0	0	4	0	1	0
<i>SA</i>	4	0	1	0	3	0	1	0	50	0	4	1
<i>SD</i>	1	0	1	0	1	0	0	0	14	0	3	0
<b>Intronic</b>	<b>1,382</b>	<b>13</b>	<b>42</b>	<b>26.5</b>	<b>1,558</b>	<b>17</b>	<b>57</b>	<b>30.5</b>	<b>19,202</b>	<b>288</b>	<b>504</b>	<b>376</b>
<i>of known ID genes</i>	34	0	4	0	<i>n.a</i>	<i>n.a</i>	<i>n.a</i>	<i>n.a</i>	<i>n.a</i>	<i>n.a</i>	<i>n.a</i>	<i>n.a</i>
<b>UTR</b>	<b>193</b>	<b>0</b>	<b>11</b>	<b>3.5</b>	<b>206</b>	<b>0</b>	<b>13</b>	<b>4</b>	<b>2525</b>	<b>7</b>	<b>82</b>	<b>61.5</b>
<i>of known ID genes</i>	6	0	2	0	<i>n.a</i>	<i>n.a</i>	<i>n.a</i>	<i>n.a</i>	<i>n.a</i>	<i>n.a</i>	<i>n.a</i>	<i>n.a</i>
<b>MicroRNA</b>	<b>0</b>	<b>0</b>	<b>0</b>	<b>0</b>	<b>1</b>	<b>0</b>	<b>1</b>	<b>0</b>	<b>2</b>	<b>0</b>	<b>1</b>	<b>0</b>
<b>Non-genic</b>	<b>2,422</b>	<b>31</b>	<b>69</b>	<b>48</b>	<b>3,184</b>	<b>41</b>	<b>90</b>	<b>63</b>	<b>40,151</b>	<b>590</b>	<b>964</b>	<b>813.5</b>

Statistics of de novo mutations identified across 50 trios. De novo calls were categorized in three confidences (see supplementary methods). Top row column header indicates the confidence category; second row column header indicates for each category the total number, the minimum number, the maximum number and the median of variants identified across all 50 trios. Rows indicate functional categorization of variants based on their location in the genome. Splice sites are divided into splice acceptor (SA) and splice acceptor (SD) canonical, being the first two bases into the intron as well as the complete splice acceptor being 20 bp within the intron and the complete splice

**Supplementary Table 5: Validation rates of autosomal candidate de novo SNVs grouped by genomic location and confidence level**

	Confidence			
	Low	Medium	High	Total
<b>Coding</b>	4/139	17/82	59/80	<b>80/301</b> (27%)
<b>Splice sites*</b>	0/15	1/6	4/6	<b>5/27</b> (19%)
<b>Intronic</b>	<i>n.a.</i>	<i>n.a.</i>	42/46	<b>42/46</b> (91%)
<b>UTR</b>	<i>n.a.</i>	<i>n.a.</i>	3/7	<b>3/7</b> (42%)
<b>Promoter</b>	<i>n.a.</i>	<i>n.a.</i>	1/1	<b>1/1</b> (100%)
<b>Total</b>	<b>4/154</b> (3%)	<b>18/88</b> (20%)	<b>109/140</b> (78%)	<b>131/382</b> (34%)

*n.a.* = not assessed. \*includes canonical splice sites.

***Supplementary Table 6: Distribution of de novo SNVs in coding sequence identified through WGS***

	Number of patients (WGS)
<b>Mutation Negative</b>	<b>9</b>
<i>0 mutations</i>	<i>9</i>
<b>Mutation Positive</b>	<b>41</b>
<i>1 mutation</i>	<i>15</i>
<i>2 mutations</i>	<i>14</i>
<i>3 mutations</i>	<i>8</i>
<i>4 mutations</i>	<i>3</i>
<i>5 mutations</i>	<i>1</i>

***Supplementary Table 7: De novo substitution rates and type of mutations identified through WGS***

	Number of mutations WGS
<b>Synonymous</b>	<b>19</b>
Predicted effect on splicing	4
No predicted effect on splicing	15
<b>Non-synonymous</b>	<b>65</b>
Nonsense	10
Missense	49
Insertion/deletion	5
Canonical splice site	1
<b><i>De novo</i> mutation rate<sup>*</sup></b>	<b>1.58</b>

*\*Calculation of the de novo mutation rate is based on substitutions only.*

**Supplementary Table 8: Coding de novo SNVs identified in 50 patients with severe ID**

Trio	Gene	Genomic annotation	cDNA	Protein	Mutation type	predicted effect on splicing? <sup>#</sup>	Gene status	Functional evaluation	Nature of mutation	Prediction software	Genomic Location	Expression pattern	Enrichment for gene ontology	Analysis of Mouse phenotypes	Diagnostic interpretation of individual variants
1	NGFR	Chr17(GRCh37):g.47583816T>C	NM_002507.3:c.364T>C	p.Cys122Arg	Missense	-		F	P	C	B	G	M		Candidate
2	GFPT2	Chr5(GRCh37):g.179728574G>C	NM_005110.2:c.2039C>G	p.Thr680Ser	Missense	-		F	P	C	B	G			Candidate
2	TRIO	Chr5(GRCh37):g.14390384A>T	NM_007118.2:c.4103A>T	p.Asp1368Val	Missense	-	K <sup>#</sup>	F				B	G	M	NO*
3	C15orf40	Chr15(GRCh37):g.83677401C>T	NM_001160115.1:c.265G>A	p.Ala89Thr	Missense	-				P					NO
3	RB1	Chr13(GRCh37):g.48921977T>C	NM_000321.2:c.517T>C	p.Tyr173His	Missense	-				P		B	G	M	NO
3	SSPO	Chr7(GRCh37):g.149487581G>T	NM_198455:c.4895G>T	p.Gly1632Val	Missense	-		F							NO
3	USP42	Chr7(GRCh37):g.6196670C>G	NM_032172.2:c.3927C>G	p.Leu1309Leu	Synonymous	-						u		M	NO
4	CNGA3	Chr2(GRCh37):g.99012638G>T	NM_001298.2:c.1005G>T	p.Trp335Cys	Missense	-				P	C	B	G	M	NO
4	CXXC11	Chr2(GRCh37):g.242814942G>A	NM_173821.2:c.1235G>A	p.Gly412Asp	Missense	-				P		B			NO
4	LPPR3	Chr19(GRCh37):g.815253C>T	NM_024888.1:c.336G>A	p.Ala112Ala	Synonymous	no		F				u			NO
6	CDC5L	Chr6(GRCh37):g.44392245C>T	NM_001253.2:c.1494C>T	p.Ala498Ala	Synonymous	no						B			NO
6	POP1	Chr8(GRCh37):g.99142350C>T	NM_001145860.1:c.631C>T	p.Arg211Trp	Missense	-		F	P						NO
6	WWP2	Chr16(GRCh37):g.69820943A>T	NM_007014.3:c.30A>T	p.Gly10Gly	Synonymous	possibly		F	D			B	G		Candidate
7	CLRN3	Chr10(GRCh37):g.129690984A>T	NM_152311.3:c.65T>A	p.Ile22Asn	Missense	-				P					NO
7	OSBPL9	Chr1(GRCh37):g.52231512C>T	NM_148909.3:c.827C>T	p.Pro276Leu	Missense	-				P	C	B			NO
7	OTX2	Chr14(GRCh37):g.57268586G>T	NM_021728.2:c.761C>A	p.Ser254*	Nonsense	-		F	D			B	G	M	NO**
7	TBR1	Chr2(GRCh37):g.16227551A>G	NM_006593.2:c.1118A>G	p.Gln373Arg	Missense	-	K	F		P	C	B	G	M	Known
7	YTHDC1	Chr4(GRCh37):g.69203353T>C	NM_001031732.2:c.396A>G	p.Lys132Lys	Synonymous	no						B			NO
8	CNOT1	Chr16(GRCh37):g.58564225C>A	NM_016284.3:c.6204G>T	p.Leu2068Leu	Synonymous	no	K <sup>#</sup>					B	G		NO*



9	CARD8	Chr19(GRCh37):g.48734215G>A	NM_001184900.1:c.591C>T	p.Leu197Leu	Synonymous	no						B		NO
9	ELP2	Chr18(GRCh37):g.33713240C>T	NM_018255.1:c.178C>T	p.Arg60*	Nonsense	-	K <sup>#</sup>	F	D			B		NO***
9	WDR45	ChrX(GRCh37):g.48932518del	NM_007075.3:c.1030del	p.Cys344Alafs*67	Frameshift	-	K	F	D			B		Known
10	LIPI	Chr21(GRCh37):g.15535845C>T	NM_198996.2:c.965-1G>A	-	Splice site	possibly							G M	NO
10	MFAP3	Chr5(GRCh37):g.153429439A>G	NM_005927.4:c.157A>G	p.Ser53Gly	Missense	-						B		NO
13	FHDC1	Chr4(GRCh37):g.153884006G>C	NM_033393.2:c.891G>C	p.Leu297Phe	Missense	-		F		P		B		NO
13	FHOD1	Chr16(GRCh37):g.67281195G>A	NM_013241.2:c.119C>T	p.Ala40Val	Missense	-					C			NO
13	SMC1A	ChrX(GRCh37):g.53430554del	NM_006306.2:c.2364del	p.Asn788Lysfs*10	Frameshift	-	K	F	D			B	G M	Known
13	ZNF566	Chr19(GRCh37):g.36940271C>T	NM_001145345.1:c.865G>A	p.Gly289Arg	Missense	-				P	C	B		NO
14	GPR52	Chr1(GRCh37):g.174417259T>G	NM_005684.4:c.10T>G	p.Ser4Ala	Missense	-						B		NO
15	DSP	Chr6(GRCh37):g.7583973C>T	NM_004415.2:c.6478C>T	p.Arg2160*	Nonsense	-			D				M	NO
15	PTPN21	Chr14(GRCh37):g.88945321C>T	NM_007039.3:c.2454G>A	p.Pro818Pro	Synonymous	no								NO
15	SPTAN1	Chr9(GRCh37):g.131331084G>A	NM_001130438.2:c.271G>A	p.Glu91Lys	Missense	-	K	F		P	C	B	G M	Known
17	ASUN	Chr12(GRCh37):g.27087494G>A	NM_018164.2:c.295C>T	p.Gln99*	Nonsense	-		F	D			B		Candidate
17	PI4K2B	Chr4(GRCh37):g.25236025G>C	NM_018323.3:c.240G>C	p.Glu80Asp	Missense	-								NO
19	TBKBP1	Chr17(GRCh37):g.45786784A>C	NM_014726.2:c.1685A>C	p.His562Pro	Missense	-						B		NO
20	SON	Chr21(GRCh37):g.34923418_34923419del	NM_138927.1:c.1881_1882del	p.Val629Alafs*56	Frameshift	-		F	D			B	u	NO
21	ALG13	ChrX(GRCh37):g.110928268A>G	NM_001099922.2:c.320A>G	p.Asn107Ser	Missense	-	K <sup>#</sup>	F		P		B	G M	Known****
21	CBLB	Chr3(GRCh37):g.105421227G>A	NM_170662.3:c.1670C>T	p.Pro557Leu	Missense	-				P	C	B	M	NO
21	KRT32	Chr17(GRCh37):g.39623313C>T	NM_002278.3:c.265G>A	p.Glu89Lys	Missense	-				P				NO
21	RAI1	Chr17(GRCh37):g.17696524C>T	NM_030665.3:c.262C>T	p.Gln88*	Nonsense	-	K	F	D			B	G M	Known
22	HADHA	Chr2(GRCh37):g.26457124C>T	NM_000182.4:c.414G>A	p.Val138Val	Synonymous	no						B	G M	NO
22	MED13L	Chr12(GRCh37):g.116435026T>C	NM_015335.4:c.2579A>G	p.Asp860Gly	Missense	-	K <sup>#</sup>	F		P	C	B		Known
23	POLQ	Chr3(GRCh37):g.121208286C>T	NM_199420.3:c.3492G>A	p.Glu1164Glu	Synonymous	no								NO
23	ZNF831	Chr20(GRCh37):g.57829608G>A	NM_178457.1:c.4844G>A	p.Arg161His	Missense	-				P		u		NO
24	BRD3	Chr9(GRCh37):g.136913290A>G	NM_007371.3:c.1001T>C	p.Phe334Ser	Missense	-		F		P	C	B		Candidate
24	SEZ6	Chr17(GRCh37):g.27286180C>T	NM_178860.4:c.1970G>A	p.Arg657Gln	Missense	possibly		F				B	G M	NO
24	TNIP3	Chr4(GRCh37):g.122078277A>G	NM_001128843.1:c.335T>C	p.Leu112Pro	Missense	-								NO

25	SATB2	Chr2(GRCh37):g.200213667_200213668ins GTTGCCTTACAA	NM_001172517.1:c.929_930insTTGTA AGGCAAC	p.Gln310delinsHis CysLys AlaThr	Insertion	no	K	F	D		C	B	G	M	Known
26	ELMO2	Chr20(GRCh37):g.45022193C>A	NM_133171.3:c.167G>T	p.Gly56Val	Missense	-				P	C	B			NO
26	PPP2R5D	Chr6(GRCh37):g.42975030T>A	NM_006245.2:c.619T>A	p.Trp207Arg	Missense	-	K <sup>#</sup>	F		P	C	B	G	M	Known
27	CATSPERB	Chr14(GRCh37):g.92136238G>T	NM_024764.2:c.1207C>A	p.Arg403Arg	Synonymous	possibly									NO
27	KCNA1	Chr12(GRCh37):g.5021656C>T	NM_000217.2:c.1112C>T	p.Thr371Ile	Missense	-	K	F		P	C	B	G	M	Known
27	SPACA7	Chr13(GRCh37):g.113030776C>T	NM_145248.4:c.77C>T	p.Pro26Leu	Missense	-						u			NO
28	DOK4	Chr16(GRCh37):g.57513380C>A	NM_018110.3:c.40G>T	p.Val14Leu	Missense	-		F			C	B	G		NO
28	SCN2A	Chr2(GRCh37):g.166243265C>T	NM_001040142.1:c.4561C>T	p.Gln1521*	Nonsense	-	K	F	D			B	G	M	Known
29	USP8	Chr15(GRCh37):g.50790871G>A	NM_001128611.1:c.3117G>A	p.Gln1039Gln	Synonymous	no						B			NO
30	MAST1	Chr19(GRCh37):g.12984501C>G	NM_014975.2:c.3530C>G	p.Pro1177Arg	Missense	-		F		P	C	B	G		Candidate
30	NEK1	Chr4(GRCh37):g.170359295T>G	NM_001199397.1:c.2703A>C	p.Lys901Asn	Missense	-						B		M	NO
32	PNLIPRP1	Chr10(GRCh37):g.118354347C>T	NM_006229.2:c.436C>T	p.Gln146*	Nonsense	-			D			G			NO
33	CDC34	Chr19(GRCh37):g.541442G>A	NM_004359.1:c.601G>A	p.Glu201Lys	Missense	-	F					B			NO
33	FAM46B	Chr1(GRCh37):g.27339042G>A	NM_052943.3:c.120C>T	p.Ala40Ala	Synonymous	no	-								NO
34	APPL2	Chr12(GRCh37):g.105591609G>C	NM_018171.3:c.986C>G	p.Ser329*	Nonsense	-	F	D				B	G	M	Candidate
34	SMAD6	Chr15(GRCh37):g.66995638G>A	NM_005585.4:c.42G>A	p.Trp14*	Nonsense	-			D					M	NO
34	ZNF423	Chr16(GRCh37):g.49670125T>C	NM_015069.3:c.2938A>G	p.Thr980Ala	Missense		F					B			NO
36	ATP7B	Chr13(GRCh37):g.52536008G>A	NM_000053.3:c.1911C>T	p.Asn637Asn	Synonymous	no						B	G	M	NO
36	CEP170B	Chr14(GRCh37):g.105352391G>C	NM_001112726.2:c.1959G>C	p.Pro653Pro	Synonymous	no						u			NO
37	PIAS1	Chr15(GRCh37):g.68468014T>A	NM_016166.1:c.1209T>A	p.Asp403Glu	Missense	-	K <sup>#</sup>	F				u	G		NO*
38	GIPC2	Chr1(GRCh37):g.78511993G>T	NM_017655.4:c.215G>T	p.Gly72Val	Missense	-									NO
39	EFS	Chr14(GRCh37):g.23829243G>A	NM_005864.2:c.444C>T	p.Tyr148Tyr	Synonymous	no						B			NO
40	ZFYVE16	Chr5(GRCh37):g.79733643C>T	NM_014733.3:c.1139C>T	p.Ala380Val	Missense	no						B	G		NO
41	CLSTN3	Chr12(GRCh37):g.7295875C>T	NM_014718.3:c.1815C>T	p.Gly605Gly	Synonymous	no	F					B			NO
41	NACC1	Chr19(GRCh37):g.13249038C>T	NM_052876.2:c.1402C>T	p.Arg468Cys	Missense	-	F				C	B			Candidate
42	HIVEP2	Chr6(GRCh37):g.143092683C>T	NM_006734.3:c.3193G>A	p.Ala1065Thr	Missense	-	K <sup>#</sup>	F				B			NO*
43	C20orf26	Chr20(GRCh37):g.20243639A>C	NM_015585.3:c.2368A>C	p.Thr790Pro	Missense	-				P	C	B			NO
43	EYA4	Chr6(GRCh37):g.133777699C>G	NM_004100.4:c.283C>G	p.Leu95Val	Missense	-	K <sup>#</sup>				C			M	NO*

43	POGZ	Chr1(GRCh37):g.151378510G>A	NM_015100.3:c.3001C>T	p.Arg1001*	Nonsense	-	K <sup>#</sup>	F	D	B				Known
44	RBL2	Chr16(GRCh37):g.53472982G>T	NM_005611.3:c.295G>T	p.Val99Phe	Missense	-								
46	CREBL2	Chr12(GRCh37):g.12788868G>C	NM_001310.2:c.173G>C	p.Arg58Pro	Missense	-								
46	TBR1	Chr2(GRCh37):g.162280277_162280283dup	NM_006593.2:c.1588_1594dup	p.Thr532Argfs*144	Frameshift	-	K	F	D		B	G	M	Known
47	ABCC8	Chr11(GRCh37):g.17483205G>A	NM_000352.3:c.747C>T	p.Ala249Ala	Synonymous	no					B	G		NO
48	EPHB1	Chr3(GRCh37):g.134514481T>G	NM_004441.4:c.8T>G	p.Leu3Arg	Missense	-		F			B	G	M	NO
48	UCP1	Chr4(GRCh37):g.141489817C>T	NM_021833.4:c.67G>A	p.Ala23Thr	Missense	-						G	M	NO
49	ERV3-1	Chr7(GRCh37):g.64452368A>C	NM_001007253.3:c.1037T>G	p.Ile346Ser	Missense	-					B			NO
49	KANSL2	Chr12(GRCh37):g.49072911C>A	NM_017822.3:c.453G>T	p.Gly151Gly	Synonymous	possibly	K <sup>#</sup>	F	D		C	u		Known

K: Known ID gene; K<sup>#</sup>: Candidate ID gene; F: Functional link to ID; D: deleterious mutation; P: Predicted pathogenic mutation; C: Conserved genomic location (not assessed for deleterious mutations); B: Brain expressed; G: Annotated with GO BP terms that are enriched in known ID genes; M: Annotated with mouse phenotypes that are enriched in known ID genes.\*Despite being a mutation in a candidate ID gene, this mutation is not considered the cause of ID as the mutation impact on protein function is not (predicted) pathogenic. \*\*: the OTX2 mutation in this patient is not diagnostically reported as cause of ID due to the classical phenotype for OTX2 mutations not being observed (ocular anomalies and pituitary deficiency). Alternatively, the phenotypic consequences of the OTX2 mutation in this patient may be atypic and superseded by the de novo TBR1 mutation. \*\*\*ELP2 mutations are known for autosomal recessive ID.<sup>77</sup> In this patient, no second (inherited) pathogenic mutation was encountered, suggesting that this mutation creates a carrier ship rather than a cause for disease. This explanation is further supported by the fact that the patient has a pathogenic mutation in WDR45, fully explaining the patients phenotype. \*\*\*\*: Additional ALG13 mutations have been reported in patients with ID since selection of this patient cohort.<sup>46,78</sup>; In retrospect, this mutation may have clinical consequences. Nonetheless, a nonsense mutation in RAI1 has been identified in the same patient during this study, which seemingly explains the full phenotype of the patient. Alternatively, the phenotype due to the ALG13 mutation may be merged into the RAI1 phenotype, making it impossible to distinguish which part of the phenotype is caused by which mutation. This phenomenon, that two (de novo) pathogenic mutations are identified in a single patient has been described before.<sup>79</sup>

**Supplementary Table 9: Coding de novo mutation rates of published studies**

Study	Number of individuals	Patients/ Controls	Disease*	# de novo SNVs excl indels	# de novo SNVs incl indels	Coding mutation rate SNVs excl indels	Coding mutation rate SNVs incl indels
<b>This study</b>	50	Patients	ID	79	84	1.58	1.68
<b>Rauch et al.<sup>32</sup></b>	51	Patients	ID	72	85	1.41	1.67
<b>O'Roak et al.<sup>33</sup></b>	189	Patients	ASD	225	242	1.19	1.28
<b>Epi4K<sup>46</sup></b>	264	Patients	EE	309	329	1.17	1.25
<b>Jiang et al.<sup>34</sup></b>	32	Patients	ASD	36	38	1.13	1.19
<b>Rauch et al.<sup>32</sup></b>	20	Controls	-	22	23	1.10	1.15
<b>Neale et al.<sup>17</sup></b>	175	Patients	ASD	161	167	0.92	0.95
<b>Gulsuner et al.<sup>51</sup></b>	105	Patients	SCHZ	96	103	0.91	0.98
<b>Iossifov et al.<sup>31</sup></b>	343	Patients	ASD	305	305	0.89	0.89
<b>Iossifov et al.<sup>31</sup></b>	343	Controls	-	294	294	0.86	0.86
<b>Gulsuner et al.<sup>51</sup></b>	84	Controls	-	66	67	0.79	0.80
<b>de Ligt et al.<sup>2</sup></b>	100	Patients	ID	72	79	0.72	0.79
<b>Sanders et al.<sup>30</sup></b>	238	Patients	ASD	164	167	0.69	0.70
<b>Xu et al.<sup>53</sup></b>	53	Patients	SCHZ	36	40	0.68	0.75
<b>Sanders et al.<sup>30</sup></b>	200	Controls	-	125	125	0.63	0.63
<b>Xu et al.<sup>53</sup></b>	22	Controls	-	8	8	0.36	0.36

\*: ID: Intellectual Disability; EE: Epileptic Encephalopathies; SCHZ: Schizophrenia; ASD: Autism Spectrum Disorder

**Supplementary Table 10: List of 528 known ID genes used for prioritization of variants**

Gene										
ABCC9	ASXL1	CHD7	ERCC5	GPC3	KIF11	MTR	PAFAH1B1	PYCR1	SLC35C1	TNK2
ABCD1	ATP1A2	CHKB	ERCC6	GPHN	KIF7	MTRR	PAK3	RAB18	SLC4A4	TOR1A
ABCD4	ATP2A2	CHRNA2	ERCC8	GPR56	KIRREL3	MUT	PANK2	RAB27A	SLC6A3	TPK1
ABHD5	ATP6V0A2	CLCN7	ESCO2	GRIA3	KIT	MVK	PARP1	RAB3GAP1	SLC6A8	TPO
ACAD9	ATP7A	CLN8	ETFB	GRIN2A	KNCQ2	MYCN	PAX6	RAB3GAP2	SLC7A7	TRAPPC9
ACOX1	ATR	CNTNAP2	ETHE1	GRIN2B	KRAS	MYH9	PC	RAF1	SLC9A6	TREX1
ACSF3	ATRX	COG8	EXOSC3	GRM1	L1CAM	MYO1E	PCDH19	RAI1	SMAD4	TRIM32
ACTB	ATXN1	COL4A1	EXT1	GSS	L2HGDH	MYO3A	PCNT	RARS2	SMARCA2	TRPM6
ACTG1	AUH	COL4A2	FAM123B	GUSB	LAMA2	MYT1L	PDE4D	RASGEF1B	SMARCA4	TSC1
ACVR1	AUTS2	COLEC11	FANCB	HAX1	LAMC3	NAGA	PDHA1	RBFOX1	SMARCB1	TSC2
ADAR	B3GALT1	COQ2	FANCD2	HCCS	LAMP2	NAGLU	PEPD	RFT1	SMARCE1	TSPAN7
ADCK3	BBS1	CREBBP	FBN1	HCFC1	LARGE	NBN	PEX1	RFX3	SMC1A	TTC8
ADSL	BBS10	CTNNA1	FGD1	HDAC4	LCT	NDE1	PEX10	RNASEH2A	SMOC1	TTN
AFF2	BBS12	CUBN	FGFR2	HDAC8	LIG4	NDP	PEX13	RNASEH2B	SMPD1	TUBA1A
AGA	BBS2	CUL3	FGFR3	HESX1	LRP1	NDUFS1	PEX26	RNASEH2C	SMS	TUBB2B
AGPAT2	BBS4	CUL4B	FH	HLCS	LRP2	NDUFS2	PEX5	ROGDI	SNAP29	TUSC3
AGTR2	BBS5	CYBSR3	FKBP	HMGGA2	MAN2B1	NDUFS4	PEX7	RP2	SOS1	TWIST1
AHCY	BBS7	D2HGDH	FKTN	HNRNP1	MANBA	NDUFS8	PGAP2	RPGRIP1L	SOX10	UBE2A
AHI1	BBS9	DARS2	FLG	HOXA1	MAP2K1	NDUFV1	PGK1	RPS6KA3	SOX2	UBE3A
AK1	BCKDHA	DBT	FLNA	HPD	MAP2K2	NEDD4L	PHF21A	RTEL1	SOX3	UBR1
AKT3	BCKDHB	DCX	FMR1	HPRT1	MAPT	NEU1	PHF6	RUNX1	SOX5	UPB1
ALDH18A1	BCOR	DDHD2	FOXG1	HRAS	MAT1A	NF1	PHF8	RYR1	SPG7	UPF3B
ALDH3A2	BCS1L	DHCR24	FOXP1	HSD17B10	MBD5	NFIA	PHGDH	RYR2	SPRED1	VLDLR
ALDH5A1	BLM	DHCR7	FOXP2	HUWE1	MBTPS2	NFIX	PIGV	SALL1	SPTAN1	VPS13B
ALG1	BRAF	DISC1	FRAS1	IDS	MCCC1	NHS	PLCB1	SATB2	SRCAP	VPS39
ALG12	BSCL2	DKC1	FTO	IDUA	MCCC2	NIPBL	PLP1	SBF1	SRD5A3	WDR11
ALG3	BUB1B	DLD	FTSJ1	IFT172	MCOLN1	NKX2-1	PMM2	SCN1A	SRGAP3	WDR19
ALG6	C5ORF42	DLG3	FUCA1	IGF1	MCPH1	NLGN1	PNKP	SCN2A	STRA6	WDR45
AMT	C7orf11	DMD	GABRA1	IKBK	MECP2	NLGN4X	PNP	SCN8A	STS	WDR62
ANK2	CA2	DNAH5	GABRB3	IL1RAPL1	mecp2e1	NLRP3	POLG	SCO2	STXBP1	XPA
ANK3	CACNA1A	DNMT3B	GALE	INPP5E	MED12	NOG	POLR3A	SDHA	SUCLA2	YWHA
ANKH	CACNA1C	DOCK8	GALT	IQSEC2	MEF2C	NOTCH3	POLR3B	SERAC1	SUOX	ZDHHC9
ANKRD11	CASK	DPAGT1	GAMT	IRS1	MGAT2	NPHP1	POMGNT1	SETBP1	SURF1	ZEB2
ANO5	CBS	DPM1	GATM	ISPD	MID1	NR0B1	POMT1	SHANK2	SYN1	ZFH4
ANTXR1	CC2D2A	DPYD	GCH1	ITGB3	MKKS	NR4A2	POMT2	SHANK3	SYNE1	ZFYVE26
AP1S2	CCBE1	DYM	GDI1	ITPR1	MLH1	NRXN1	PORCN	SHH	SYNGAP1	ZIC2
AP3B1	CCDC22	DYNC1H1	GFAP	KANK1	MLL	nrxn1b	POU1F1	SHOC2	SYP	ZNF41
APAF1	CCDC39	DYRK1A	GJC2	KANSL1	MLL2	NSD1	POU3F4	SHOX	TAT	ZNF674
APTX	CDH15	EFTUD2	GK	KAT6B	MLL3	NSDHL	PPM1D	SHROOM4	TBC1D24	
ARFGEF2	CDK5RAP2	EHMT1	GLDC	KCNA1	MLYCD	NSUN2	PPOX	SIL1	TBR1	
ARHGEF9	CDKL5	EIF2AK3	GLI2	KCNJ10	MMAA	NTRK1	PRODH	SIX3	TCF4	
ARID1A	CDON	EIF4G1	GLI3	KCNJ11	MMACHC	OBSL1	PRPS1	SKI	TFAP2A	
ARID1B	CELSR1	ELOVL4	GLRA1	KCNQ2	MMADHC	OCA2	PSEN1	SLC12A6	TGFBR1	

<i>ARL6</i>	<i>CENPJ</i>	<i>EP300</i>	<i>GMPPB</i>	<i>KCNQ3</i>	<i>MOCS1</i>	<i>OCLN</i>	<i>PTCH1</i>	<i>SLC16A2</i>	<i>TGFBR2</i>
<i>ARSE</i>	<i>CEP152</i>	<i>EPHA5</i>	<i>GNAS</i>	<i>KCNT1</i>	<i>MOCS2</i>	<i>OCRL</i>	<i>PTCHD1</i>	<i>SLC17A5</i>	<i>TGIF1</i>
<i>ARX</i>	<i>CEP290</i>	<i>EPHB2</i>	<i>GNPAT</i>	<i>KCTD7</i>	<i>MPDU1</i>	<i>OFD1</i>	<i>PTDSS1</i>	<i>SLC25A15</i>	<i>THRB</i>
<i>ASL</i>	<i>CEP41</i>	<i>ERBB4</i>	<i>GNRHR</i>	<i>KDM5C</i>	<i>MPDZ</i>	<i>OPHN1</i>	<i>PTEN</i>	<i>SLC26A9</i>	<i>TIMM8A</i>
<i>ASPA</i>	<i>CHAT</i>	<i>ERCC2</i>	<i>GNS</i>	<i>KDM6A</i>	<i>MSH6</i>	<i>ORC1</i>	<i>PTPN11</i>	<i>SLC2A1</i>	<i>TMEM237</i>
<i>ASPM</i>	<i>CHD2</i>	<i>ERCC3</i>	<i>GP1BB</i>	<i>KIAA1279</i>	<i>MTMR2</i>	<i>OTC</i>	<i>PVRL1</i>	<i>SLC33A1</i>	<i>TMEM67</i>

**Supplementary Table 11: List of 628 Candidate ID genes used for prioritization of variants**

Gene									
ABCA2	C16orf62	DDX11	FGD3	KIAA0317	NDUFA1	PPP2R2C	SLC25A22	TMLHE	ZNF480
ABCG4	C17orf53	DDX20	FGF22	KIAA1033	NDUFA11	PPP2R5D	SLC25A39	TMPRSS12	ZNF526
ABI3BP	C1QTNF6	DDX3X	FLVCR1	KIAA1109	NDUFA12	PQBP1	SLC25A5	TNKS2	ZNF565
ACACB	C6orf174	DDX50	FMN2	KIAA1324L	NDUFS3	PRDM12	SLC31A1	TNPO2	ZNF592
ACBD6	C7orf43	DEAF1	FREM3	KIAA1462	NDUFS7	PRDX6	SLC35A2	TNR	ZNF673
ACO2	C9orf86	DENR	FRMPD4	KIAA2018	NFASC	PRKCA	SLC4A10	TOP1	ZNF711
ACSL4	CA8	DGCR14	FRY	KIAA2022	NGEF	PRKCB	SLC4A8	TRAK1	ZNF81
ADAT3	CACNA1E	DGCR2	GABRB1	KIF14	NISCH	PRKRA	SLC6A1	TRAPPC11	
ADCY7	CACNA1G	DGKH	GAD1	KIF1A	NLGN2	PRMT10	SLC6A13	TRIM29	
ADK	CACNG2	DHDDS	GAS2	KIF5C	NLRCS	PROX2	SMARCC2	TRIM8	
ADNP	CAMK2G	DHFR	GATAD2B	KLF12	NOTUM	PRPF39	SMC3	TRIO	
ADRA2B	CAP1	DHRS4L1	GCSH	KLF8	NPAS4	PRSS12	SMG9	TRIP12	
AGPAT3	CARKD	DHTKD1	GIMAP8	KLHL11	NPRL2	PSMA7	SMURF1	TRMT1	
AIFM1	CASP2	DIAPH3	GNAO1	KPNA1	NR2F1	PSMG4	SNIP1	TRMT10A	
AIMP1	CC2D1A	DIP2B	GOLGA3	KRT80	NRN1	PTGR1	SNX3	TRPC5	
AKR1C4	CCDC137	DIP2C	GON4L	LAMA1	NTNG1	PTPRK	SOBP	TRPM3	
ALG2	CCDC18	DLG1	GPD2	LARP7	NUAK1	PTPRM	SP7	TRPM5	
ALG9	CCDC78	DLG4	GPR115	LINS	NUP54	PTPRR	SPAG17	TRPM7	
ALS2CL	CCDC8	DLL1	GPR153	LRPPRC	NXF5	PTPRT	SPATA13	TRRAP	
ALX1	CCDC84	DLX3	GPR84	LTN1	OMG	PUS1	SPATA5	TSPAN17	
AMY2B	CCNT1	DMPK	GPS1	LZTR1	OPLAH	PWWP2A	SRBD1	TSPYL5	
ANKRD12	CDC42BPB	DNAH17	GRB14	MADD	OPRL1	RAB2A	SRPR	TTI2	
ANO10	CDK11A	DNAH7	GRIA1	MAGEL2	OR10S1	RAB33B	SRPX2	TUBGCP6	
AP2A2	CDK5R1	DNAJB9	GRIA2	MAGT1	OR5M1	RAB39B	SSBP3	UBE3B	
AP3B2	CDK6	DNAJC19	GRIK2	MAN1B1	OSBPL5	RAB40AL	ST3GAL3	UBE3C	
AP3M1	CDKL3	DNAJC6	GRIN1	MAOA	PACS1	RAB5C	ST3GAL5	UBN2	
AP4B1	CDS2	DNM1	GRM5	MAPK10	PACS2	RAD21	ST3GAL6	UBQLN1	
AP4E1	CELF2	DNMT3A	GRM7	MAPK8IP1	PAFAH1B3	RAD21L1	ST5	UBR3	
AP4S1	CEP135	DOCK9	GSPT2	MBTPS1	PALLD	RALGAPB	STAG1	UBR5	
APH1A	CHAMP1	DPP3	GTF2H5	MCAM	PAX1	RALGDS	STAP2	UBR7	
ARHGAP30	CHD1	DPP7	GTPBP8	MCM3AP	PAX5	RALGPS1	STIL	UBTF	
ARHGEF10	CHD3	DRD4	H2AFV	MED13	PBRM1	RAPGEF1	STK36	UGGT1	
ARHGEF6	CHD6	DST	HARS	MED13L	PCDH11X	RARG	STT3A	UNC13C	
ARIH1	CHL1	DUS1L	HDGFRP2	MED17	PCDH18	RARS	STT3B	UNC80	
ARL13B	CHRNA7	DUSP15	HDLBP	MED23	PCDHA13	RASGRP1	STX1B	UPF2	
ARMC9	CIC	EBAG9	HDX	MEGF11	PCDHB13	RASIP1	STXBP3	URB2	
ASAH2	CIT	EDA2R	HECTD1	MEOX2	PCDHB4	RB1CC1	SUPT16H	USP15	
ASB1	CLIC2	EEF1A2	HERC2	METTL14	PCNX	RBM10	SV2B	USP46	
ASCC3	CLK2	EEF1B2	HIPK3	MGAT4C	PCOLCE	RBM28	SVIL	UTP14C	
ASCL1	CNKSR1	EFHC2	HIST1H1E	MIB1	PDCD1	RBMS3	SYNCRIP	VCX3A	
ASH1L	CNKSR2	EFR3A	HIST1H2AE	MKLN1	PDIA6	RECK	SYNRG	VPS37A	
ASNS	CNOT1	EIF2C1	HIST1H2AG	MLL4	PDIK1L	RELN	SYT14	WAC	
ATP10D	CNOT3	EIF2S3	HIST3H3	MLL5	PDSS1	REPS2	SZT2	WDFY3	
ATP12A	CNOT4	ELK1	HIVEP2	MMP27	PDSS2	REST	TAAR2	WDR13	

ATP1B1	CNTN5	ELP2	HTR7	MMP8	PECR	RGMA	TAF1	WDR45L
ATP2B4	COG1	EMILIN3	IER3IP1	MOB4	PEX11B	RGS14	TAF2	WDR62
ATP6AP2	COG6	EMX2	IFT81	MPHOSPH8	PGRMC1	RGS7	TAF7L	WHSC1L1
ATP8A2	COG7	ENTPD1	IGBP1	MPP6	PHACTR1	RIMS1	TANC2	XPO1
B3GNT4	COL25A1	EPB41L1	inpp4a	MRPS22	PHF19	RIMS2	TBC1D14	XPO5
B4GALT1	COL4A3BP	EPC2	IQGAP2	MRS2	PHF2	RIOK3	TBC1D7	XPR1
B4GALT7	COLEC12	ERLIN2	IQSEC1	MTF1	PHIP	RMND1	TBCE	XYLT1
BCAP31	COQ5	ESAM	ITGA5	MTMR12	PIAS1	RNF38	TBL1XR1	YWHAG
BCORL1	COX15	EXOC6B	JAM3	MTOR	PIGL	RREB1	TBX18	YY1
BEST3	CRADD	EYA4	JARID2	MYH10	PIGN	RRP1B	TCF7L1	ZBTB40
BIRC6	CRBN	FAAH2	KANSL2	MYO5A	PIGO	RTN4RL1	TECPR2	ZBTB41
BMP1	CRK	FAM102A	KATNAL2	MYO7B	PIGT	RUNX1T1	TECR	ZC3H12B
BRAT1	CRTAC1	FAM116B	KCNB1	MYOF	PIK3R2	RUVBL1	TFDP1	ZC3H14
BRD4	CSDE1	FAM129B	KCNH1	MYT1	PIK3R3	RXFP1	TGM3	ZCCHC12
BRPF1	CSNK1E	FAM13C	KCNK12	N6AMT1	PIWIL4	S100G	THBS1	ZCCHC8
BRSK2	CTCF	FAM45A	KCNK9	NAA10	PLA1A	SAP30BP	THOC2	ZDHHC15
BRWD1	CTDP1	FAM63B	KDM1A	NAA40	PLCL2	SC5DL	THOC6	ZFHX3
BRWD3	CTTNBP2	FAM8A1	KDM1B	NACA	PLP2	SCAF4	TLK2	ZMYM3
BTN1A1	CTTNBP2NL	FAM91A1	KDM2B	NALCN	PNPLA7	SCP2	TMC4	ZMYM6
C10orf11	CUL5	FASN	KDM5A	NAPRT1	POC1A	SDCBP2	TMCO1	ZNF238
C11orf46	CUX2	FASTKD5	KDM5B	NAV2	POGZ	SEMA4G	TMEM135	ZNF292
C12orf57	CYP4F3	FAT1	KDM6B	NBEA	POLR2A	SETD5	TMEM165	ZNF385B
C12orf65	CYTH1	FBXW9	KIAA0100	NCAPD2	POLR2M	SFPQ	TMEM231	ZNF407
C15orf38	DBR1	FCRL6	KIAA0182	NCKAP1	POLRMT	SLC16A3	TMEM41A	ZNF44
C15orf62	DCAF4	FETUB	KIAA0232	NDST1	PPP1R15B	SLC1A2	TMEM85	ZNF451



***Supplementary Table 12: Summary of de novo non-coding SNVs identified in 528 known ID genes***

Non-coding component	Number of mutations
Promoter	1
5'UTR	2
Intron	38
Non-canonical splice site	1
3'UTR	1

**Supplementary Table 13: De novo SNVs in non-coding sequence identified in patients with severe ID**

Trio	Gene	Location	Genomic annotation	cDNA	PhyloP	Predicted effect on splicing?	ENCODE annotation
1	<b>LAMA2</b>	Intron	Chr6(GRCh37):g.129635764C>T	NM_000426.3:c.3412-36C>T	-0.59	no	
6	<b>MCOLN1</b>	Intron	Chr19(GRCh37):g.7597165G>C	NM_020533.2:c.1576-1244G>C	-0.44	no	
7	<b>CNTNAP2</b>	Intron	Chr7(GRCh37):g.145833308G>T	NM_014141.5:c.97+19243G>T	0.21	no	
8	<b>GRM1</b>	Intron	Chr6(GRCh37):g.146511626C>T	NM_000838.3:c.950+30893C>T	-0.36	no	
8	<b>HDAC4</b>	Intron	Chr2(GRCh37):g.239978216T>C	NM_006037.3:c.2989-1687A>G	-0.92	no	
9	<b>LRP2</b>	Splice site	Chr2(GRCh37):g.170070389T>C	NM_004525.2:c.5827-9A>G	-0.02	no	
10	<b>LARGE</b>	5'UTR	Chr22(GRCh37):g.34159094C>A	NM_004737.4:c.-82-1549G>T	-0.42	no	
12	<b>MAP2K1</b>	Intron	Chr15(GRCh37):g.66775036A>G	NM_002755.3:c.693+819A>G	-0.20	no	
13	<b>STXBP1</b>	Intron	Chr9(GRCh37):g.130417532G>A	NM_003165.3:c.169+1457G>A	-0.40	no	
13	<b>AUH</b>	Intron	Chr9(GRCh37):g.94078475C>T	NM_001698.2:c.505+9125G>A	1.57	no	
14	<b>ACVR1</b>	Intron	Chr2(GRCh37):g.158654234G>A	NM_001105.4:c.67+1705C>T	-0.60	no	
16	<b>PNKP</b>	Intron	Chr19(GRCh37):g.50367525C>T	NM_007254.3:c.579-32G>A	-0.70	possibly	
17	<b>MCPH1</b>	Intron	Chr8(GRCh37):g.6438621C>A	NM_024596.3:c.2215-40354C>A	-0.44	no	
17	<b>GRM1</b>	Intron	Chr6(GRCh37):g.146468131A>G	NM_000838.3:c.701-12353A>G	0.04	no	
18	<b>ALG12</b>	Intron	Chr22(GRCh37):g.50298304C>T	NM_024105.3:c.993-150G>A	-2.86	no	
18	<b>GRIN2A</b>	Intron	Chr16(GRCh37):g.10168818T>C	NM_000833.3:c.414+105037A>G	0.04	no	
19	<b>VPS13B</b>	Intron	Chr8(GRCh37):g.100785479A>G	NM_017890.4:c.7323-3524A>G	0.37	no	
20	<b>FOXP1</b>	Intron	Chr3(GRCh37):g.71222718G>A	NM_001244810.1:c.180+24635C>T	0.12	no	
22	<b>NRXN1</b>	Intron	Chr2(GRCh37):g.51178159T>C	NM_001135659.1:c.872-25066A>G	0.12	no	
22	<b>NRXN1</b>	Intron	Chr2(GRCh37):g.51141214T>C	NM_001135659.1:c.931+7793A>G	-1.51	no	
22	<b>PVRL1</b>	Intron	Chr11(GRCh37):g.119583361G>T	NM_002855.4:c.79+15824C>A	-1.07	no	
24	<b>SPRED1</b>	Intron	Chr15(GRCh37):g.38603586G>A	NM_152594.2:c.208-10856G>A	-0.44	no	
25	<b>ALDH18A1</b>	5'UTR	Chr10(GRCh37):g.97416435_97416438del	NM_002860.3:c.-113_-110del	-	no	
27	<b>MMADHC</b>	Promoter	Chr2(GRCh37):g.150489713A>G	-	0.24	-	Weak Promoter; Heterochrom/lo;

Repetitive/CNV;  
WeakEnhancer

28	<b>BBS9</b>	Intron	Chr7(GRCh37):g.33191509G>A	NM_198428.2:c.113-804G>A	-0.44	no
28	<b>DPYD</b>	Intron	Chr1(GRCh37):g.97588236C>T	NM_000110.3:c.2623-24048G>A	0.93	no
33	<b>GNPAT</b>	Intron	Chr1(GRCh37):g.231397861A>G	NM_014236.3:c.439-608A>G	-1.17	no
33	<b>SMARCA4</b>	Intron	Chr19(GRCh37):g.11086322G>A	NM_001128849.1:c.-31-8475G>A	-2.30	no
36	<b>CCBE1</b>	Intron	Chr18(GRCh37):g.57124433G>T	NM_133459.3:c.554-2250C>A	-0.60	no
36	<b>NF1</b>	Intron	Chr17(GRCh37):g.29533557T>C	NM_001042492.2:c.1392+168T>C	0.36	no
38	<b>SETBP1</b>	Intron	Chr18(GRCh37):g.42569791G>A	NM_015559.2:c.4000+36486G>A	-0.04	no
38	<b>SCN8A</b>	Intron	Chr12(GRCh37):g.52189411C>T	NM_014191.3:c.4795+986C>T	-0.76	no
41	<b>NRXN1</b>	Intron	Chr2(GRCh37):g.50558625A>G	NM_001135659.1:c.3485-94517T>C	-0.28	no
41	<b>MEF2C</b>	Intron	Chr5(GRCh37):g.88123620C>T	NM_001193347.1:c.-142-3873G>A	-1.89	no
43	<b>BBS9</b>	Intron	Chr7(GRCh37):g.33549086C>T	NM_198428.2:c.2298+3829C>T	1.66	possibly
43	<b>PEPD</b>	Intron	Chr19(GRCh37):g.33980994G>A	NM_000285.3:c.442-31C>T	-0.36	no
45	<b>DLG3</b>	Intron	ChrX(GRCh37):g.69718156G>A	NM_021120.3:c.1820-214G>A	-0.12	no
48	<b>NRXN1</b>	Intron	Chr2(GRCh37):g.51078981C>T	NM_001135659.1:c.931+70026G>A	-1.10	no
49	<b>CEP290</b>	Intron	Chr12(GRCh37):g.88447045C>T	NM_025114.3:c.7129+384G>A	0.21	no
49	<b>ARID1B</b>	Intron	Chr6(GRCh37):g.157276718A>G	NM_020732.3:c.2037+20008A>G	1.50	no
50	<b>CCBE1</b>	3'UTR	Chr18(GRCh37):g.57102290C>T	NM_133459.3:c.*850G>A	0.26	miRNA binding?
50	<b>PLCB1</b>	Intron	Chr20(GRCh37):g.8327174C>T	NM_015192.2:c.178-24855C>T	0.22	no
50	<b>SHROOM4</b>	Intron	ChrX(GRCh37):g.50462314T>C	NM_020717.3:c.118-23377A>G	0.53	no

Confirmed non-coding de novo mutations. Effect on splicing was determined using Alamut software that integrates a number of prediction methods for splice signal detection as well as exonic splicing enhancer (ESE) binding site detection. Encode annotation was based on Chromatin state segments of nine human cell types (Broad ChromHMM) and transcription factor binding sites (Txn Factor ChIP).<sup>41</sup>

**Supplementary Table 14: Phenotypic comparison of patients with mutations in known and candidate ID genes**

<i>Trio</i>	Phenotype	<i>Mutation type</i>	<i>Gene</i>	Disease association	References
<b>5</b>	Severe ID, signs of autism, aggressive behavior, 2 café au lait spots, increased pain threshold.	CNV	<i>SHANK3</i> [OMIM 606232]	Phelan-McDermid syndrome is characterized by neonatal hypotonia, global developmental delay, absent to severely delayed speech, and normal to accelerated growth. Behavior characteristics include mouthing or chewing non-food items, decreased perception of pain, and autistic-like affect. Phelan-McDermid syndrome can be caused by a heterozygous contiguous gene deletion at chromosome 22q13 or by mutation in the <i>SHANK3</i> gene.	80,81
<b>7</b>	Developmental delay. No major dysmorphisms.	SNV	<i>TBR1</i> [OMIM 604616]	TBR1, a transcription factor involved in early cortical development, is a strong candidate for the intellectual disability phenotype seen in patients with 2q24.3 deletions. <i>De novo</i> mutations in <i>TBR1</i> have also been reported in individuals with autism.	49,82
<b>9</b>	ID from infancy. Regression at adult age. She showed parkinsonism and dystonia.	SNV	<i>WDR45</i> [OMIM 300526]	Neurodegeneration with brain iron accumulation (NBIA) is a group of genetic disorders characterized by abnormal iron deposition in the basal ganglia. <i>De novo</i> mutations in <i>WDR45</i> , encoding a beta-propeller scaffold protein with a putative role in autophagy, cause a distinctive NBIA phenotype. The clinical features include early-onset global developmental delay and further neurological deterioration (parkinsonism, dystonia, and dementia developing by early adulthood).	83,84

12	<p>ID without speech, autism. Hypotonia. Recurrent infection. Sleep disturbances, delayed puberty and obesity. Short stature and microcephaly. Deep set eyes, hypertelorism, large ears, large nose, short philtrum, full lips. Kyphosis, narrow hands with tapering fingers, partial cutaneous syndactyly of 2nd and 3rd toes and sandal gaps. No ophthalmologic anomalies.</p> <p>Of note, Cohen syndrome was part of the differential diagnosis. <i>VPS13B</i> was sequenced but with normal results.</p>	CNV	<i>VPS13B</i> [OMIM 216550]	Cohen syndrome is an autosomal recessive disorder characterized by a characteristic facial appearance, failure to thrive, microcephaly, progressive retinchoroidal dystrophy and high myopia, neutropenia with recurrent infections, a cheerful disposition, joint hypermobility, truncal obesity in puberty, early-onset hypotonia and moderate-profound ID.	85
13	<p>Severe ID with epilepsy. No speech. Short stature, microcephaly and enlarged ventricles and hypertrophy of the cerebellar vermis. Hypotonia, cleft palate, cataract, scoliosis and stereotypic movements. Dysmorphic features included a low frontal-temporal hairline, deep-set eyes, a flat midface, long narrow ears, a long nose with a high bridge, a short philtrum, an everted lower lip and a prominent jaw. In addition, she had scoliosis, short narrow hands, tapered fingers and several contractures.</p>	SNV	<i>SMC1A</i> [OMIM 610759]	Cornelia de Lange syndrome CdLS is a clinically and genetically heterogeneous developmental disorder. Clinical features include growth retardation, intellectual disability, limb defects, arched eyebrows, synophrys thin lips and other systemic involvement. Mutations in <i>SMC1A</i> are associated with a milder phenotype with moderate neurocognitive impairment and a paucity of major structural defects. Recently, one loss-of-function mutation was described in a female patient with developmental delay, microcephaly, congenital diaphragmatic hernia, and generalized epilepsy. Dysmorphic features included round face with arched eyebrows, short nose, smoothed philtrum, prominent jaw, clinodactyly of the 5 <sup>th</sup> fingers and camptodactyly of the 5 <sup>th</sup> finger on the right.	78,86-88
15	<p>Neonatal feeding problems, hip dysplasia. ID (IQ 50) and autism. Epicanthic folds, straight eyebrows, posteriorly rotated ears and downturned corners of the mouth. MRI of brain is not available. No epilepsy.</p>	SNV	<i>SPTAN1</i> [OMIM 613417]	Epileptic encephalopathy, early infantile, 5 (EIEE5). <i>SPTAN1</i> mutations have been reported in patients with severe ID, infantile spasms with hypsarrhythmia, hypomyelination and atrophy of various regions of the brain, including the cerebellum and brainstem. Mutations have also been reported in a patients with non-syndromic ID.	89

26	ID (dyshormonic profile; performat IQ 50, verbal 90), hypotonia, no facial dysmorphisms, progressive scoliosis, hip dysplasia, fatigue problems.	SNV	<i>PPP2R5D</i> [OMIM 601646]	Recently, we published a patient with a de novo mutation in <i>PPP2R5D</i> was identified. The patient presented with ID, absence of speech, no facial dysmorphisms, short stature, microcephaly, cataract, anxiety, autistic features and mood swings. The product of this gene belongs to the phosphatase 2A regulatory subunit B family. Protein phosphatase 2A is one of the four major Ser/Thr phosphatases, and it is implicated in the negative control of cell growth and division.	32
27	Severe ID. Epilepsy (tonic-clonic seizures), myokymia. Normal height, head circumference -2 SD. Broad based walking pattern. Narrow long face, prominent supraorbital ridges, long nose and philtrum, thin upper lip, hypodontia, long fingers and toes and narrow thorax.	SNV	<i>KCNA1</i> [OMIM 160120]	Mutations in <i>KCNA1</i> have been reported in patients with episodic ataxia and myokymia, without ID. In one report a family with persistent cerebellar dysfunction, cerebellar atrophy, and cognitive delay has been described. All affected family members had myokymia and epilepsy. Additional features included postural abnormalities, episodic stiffness and weakness.	94
28	ID. No major dysmorphisms. No epilepsy. Sleep disturbances and obsessive behaviour.	SNV	<i>SCN2A</i> [OMIM 182390]	<i>SCN2A</i> mutations have been reported in patients with early-onset infantile epileptic encephalopathy and also in patients with severe ID and auto-aggressive behavior but without epilepsy.	32,45
31	Severe ID, microcephaly, epilepsy, progressive spasticity, small hands and feet, poor vision.	CNV	<i>TENM3</i> [OMIM 610083] <i>IQSEC2</i> [OMIM 309530]	<i>IQSEC2</i> is a non-syndromic X-linked ID gene in which carrier females show normal or mild learning difficulties. Male patients, show phenotypic overlap with pathogenic mutations in <i>MECP2</i> , <i>FOXG1</i> , <i>CDKL5</i> and <i>MEF2C</i> , but may also manifest seizures, autistic-like behavior, psychiatric problems and delayed language skills. In most male patients the mutation occurred <i>de novo</i> (rather than maternally inherited). One other female patient with severe infantile spasms, profound global developmental arrest, hypsarrhythmia and severe ID, is reported to have a balanced translocation that disrupts <i>IQSEC2</i> .	45,95-97
40	Moderate ID, features of autism, anxiety, mood instability and aggressive outbursts. No evident dysmorphic features.	CNV	<i>STAG1</i> [OMIM 604358]	A <i>de novo</i> loss of function mutation was previously reported as a possible cause for ID in a patient with normal growth and head circumference.	45

43	Moderate ID, left hydronephrosis, right dysplastic kidney, severe hypermetropia, Horner syndrome, microcephaly.	SNV	<i>POGZ</i> [OMIM 614787]	Mutations in <i>POGZ</i> have been identified in patients with autism.	47,48
46	Severe hypotonia, severe motor delay and speech delay. Deficient gyration frontal region, mild periventricular white matter abnormalities	SNV	<i>TBR1</i> [OMIM 604616]	<i>TBR1</i> , a transcription factor involved in early cortical development, is a strong candidate for the intellectual disability phenotype seen in patients with 2q24.3 deletions. <i>De novo</i> mutations in <i>TBR1</i> have also been reported in individuals with autism.	49,82
48	Severe ID, severe epilepsy, Rett-like phenotype, motor handicap, severe feeding difficulties, progressive scoliosis	CNV	<i>SMC1A</i> [OMIM 610759]	Cornelia de Lange syndrome CdLS is a clinically and genetically heterogeneous developmental disorder. Clinical features include growth retardation, intellectual disability, limb defects, arched eyebrows, synophrys thin lips and other systemic involvement. Mutations in <i>SMC1A</i> are associated with a milder phenotype with moderate neurocognitive impairment and a paucity of major structural defects. Recently, one loss-of-function mutation was described in a female patient with developmental delay, microcephaly, congenital diaphragmatic hernia, and generalized epilepsy. Dysmorphic features included round face with arched eyebrows, short nose, smoothed philtrum, prominent jaw, clinodactyly of the 5 <sup>th</sup> fingers and camptodactyly of the 5 <sup>th</sup> finger on the right.	78,86-88
50	Profound ID, microcephaly, short stature, vaginal atresia, unilateral renal agenesis, cortical blindness, evident dysmorphic features, small hands and feet	CNV	Proximal 16p11.2 deletion [OMIM 611913]	Patients with the typical 600 kb 16p11 deletion can have borderline-mild ID, psychiatric disorders (80%), obesity (50%) and seizures (25%). This locus is known for its reduced penetrance (estimated at to be 47%), with the majority of CNVs occurring <i>de novo</i> (70% of cases). Eight percent of patients show additional variants expected to contribute to the phenotype. Such variant may also be expected in this patient.	98-100

**Supplementary Table 15: Molecular diagnosis per patient after WGS**

Trio	Molecular diagnosis?*	Based on [ <i>gene</i> ] ( <i>inheritance</i> )	Mutation type
1	Possible	<i>NGFR (de novo)</i>	Autosomal SNV
2	Possible	<i>GFT2 (de novo)</i>	Autosomal SNV
3	NO		
4	NO		
5	Highly likely	<i>SHANK3 (de novo)</i>	Autosomal CNV
6	Possible	<i>WWP2 (de novo)</i>	Autosomal SNV
7	Highly Likely	<i>TBR1 (de novo)</i>	Autosomal SNV
8	NO		
9	Highly likely	<i>WDR45 (de novo)</i>	X-linked SNV
10	NO		
11	NO		
12	Highly likely	<i>VPS13B (inherited)</i>	Autosomal CNV
13	Highly likely	<i>SMC1A (de novo)</i>	X-linked SNV
14	NO		
15	Highly likely	<i>SPTAN (de novo)</i>	Autosomal SNV
16	NO		
17	Possible	<i>ASUN (de novo)</i>	Autosomal SNV
18	Highly likely	<i>MECP2 (de novo)</i>	X-linked CNV
19	NO		
20	NO		
21	Highly likely	<i>RAI1 (de novo)</i>	Autosomal SNV
22	Highly likely	<i>MED13L (de novo)</i>	Autosomal SNV
23	NO		
24	Possible	<i>BRD3 (de novo)</i>	Autosomal SNV
25	Highly likely	<i>SATB2 (de novo)</i>	Autosomal SNV
26	Highly likely	<i>PPP2R5D (de novo)</i>	Autosomal SNV
27	Highly likely	<i>KCNA1 (de novo)</i>	Autosomal SNV
28	Highly likely	<i>SCN2A (de novo)</i>	Autosomal SNV
29	NO		
30	Possible	<i>MAST1 (de novo)</i>	Autosomal SNV
31	Highly likely	<i>IQSEC2 (de novo)</i>	Autosomal CNV/ X-linked
32	NO		
33	NO		
34	Possible	<i>APPL2 (de novo)</i>	Autosomal SNV
35	NO		
36	NO		
37	Highly likely	multiple ( <i>de novo</i> )*	Autosomal CNV
38	NO		
39	NO		
40	Highly likely	<i>STAG1 (de novo)</i>	Autosomal CNV
41	Possible	<i>NACC1 (de novo)</i>	Autosomal SNV



42	NO		
43	Highly likely	<i>POGZ (de novo)</i>	Autosomal SNV
44	NO		
45	NO		
46	Highly likely	<i>TBR1 (de novo)</i>	Autosomal SNV
47	NO		
48	Highly likely	<i>SMC1A (de novo)</i>	X-linked CNV
49	Highly likely	<i>KANSL2 (de novo)</i>	Autosomal SNV
50	Highly likely	16p11.2 microdeletion syndrome ( <i>de novo</i> )	Autosomal CNV

*\*Of note, a possible diagnosis was made in 8 patients who showed severe de novo SNVs in genes with functional support for ID-related disorders (Extended Data Table 2). Interestingly these 8 genes showed a significantly lower tolerance for normal variation similar to our set of known and candidate ID genes ( $P=0.003$ , Extended Data Figure 1). Nonetheless, conclusive diagnoses for these 8 patients cannot be made based on single observations and are thus not included in the calculated diagnostic yields. \*\*48 genes are affected by the rearrangement – phenotype may be the effect of a single dosage sensitive gene in this CNV or it may reflect a contiguous gene syndrome, with multiple genes contributing.*